THE HYDROLOGY OF A SLOPING FRAGIAQUALF

A thesis presented in partial fulfilment of
the requirements for the degree of
Master of Philosophy in Soil Science,
Massey University.

Michael Patrick Tuohy

1989

ABSTRACT

A field experiment was conducted on a sloping Tokomaru silt loam (Typic Fragiaqualf). This soil has a permeable topsoil, but is underlain with an impermeable fragipan at 500 - 700 mm. Paired runoff plots (100 m^2 in area) were constructed, and over a four-year period, rainfall, water table levels and runoff were monitored. Infiltration and saturated hydraulic conductivity were also measured. During the study period, forty surface runoff events occurred with most of these being relatively minor events where less than 1 mm of runoff was generated. Subsurface flow rather than overland flow removed most of the excess rain over winter and early spring.

The dominant surface-runoff-generating process was found to be saturation overland flow. Hortonian runoff only occurred when the infiltration capacity was reduced by pugging of the soil surface. When such a treatment was applied to one of the plots, the saturated hydraulic conductivity of the topsoil was reduced from 500 - 1200 mm/day to only 0.8 mm/day. For the damaged plot, 25% (1.8 mm) of the 7.2 mm of rain which fell over a seven hour period became overland flow. This compared to 18% (1.3 mm) of the rain becoming surface runoff on the undamaged plot.

Aspects of modelling and simulation are discussed and several rainfall-runoff models are reviewed. A simple, physically-based, finite-difference model for predicting water table behaviour and runoff generation is described. The model uses the Dupuit-Forchheimer assumptions for flow below the water table, and it assumes a constant hydraulic potential between the water table and the surface.

Water table behaviour during and following a rainstorm was predicted reasonably accurately. Using hourly rainfall data, the occurrence and magnitude of runoff surface events over a winter/spring period were simulated. The model was also used to illustrate the importance of slope angle in subsurface flow and runoff generation. Over a winter/spring period, a 100 m^2 plot with a 10% slope was predicted to have nine days on which overland flow occurred, and subsurface flow rates which sometimes exceeded 30 mm/day. For the same period, a plot with a 2% slope was shown to have much less subsurface flow (with rates not exceeding 10 mm/day), and nineteen days of surface runoff.

ACKNOWLEDGEMENTS

I would like to thank the following people whose support, guidance and friendship have helped make this thesis possible:

Dr. Dave Scotter, Department of Soil Science, and Dr. Brent Clothier, Plant Physiology Division, DSIR, for their supervision and direction.

Kevin Harris, Martin Lewis, Anne Sutherland and Sean O'Connor for their invaluable technical assistance.

Other members of the Department of Soil Science and colleagues at the DSIR who have contributed in many different ways.

Ann Rouse who has so ably typed this manuscript.

Sue, Dan and Paddy - my best mates.

TABLE OF CONTENTS

LIST OF FIGURES

LIST OF PLATES

LIST OF TABLES

CHAPTER 1

INTRODUCTION

A great deal of New Zealand's hill country consists of shallow, permeable topsoils overlying less permeable subsoils, which in turn are underlain by almost impermeable layers. The ultimate barriers to water percolation in the soil are most commonly the parent rocks from which the soils are derived. These are mainly mudstones and siltstones, but they can also be compacted gravels or conglomerates, and in soils derived from loess, a densely compacted fragipan.

The hydrological processes occurring on such hillsides are the subject of this study. During dry periods the hill-soils hold very little water and the perennial streams are barely flowing. In summer therefore, pasture growth is often restricted by a lack of water.

The autumn and early winter rains are mostly soaked up by the soil and, in general, have little immediate effect on streamflow. Once the soil wets up again, usually by mid-winter, the mechanism whereby the soil is able to regulate the amount of water entering the watercourses becomes less effective. The reservoir becomes replete, and further rain proceeds directly to the streams causing posssible flooding and erosion during large storms.

In many hill country areas it has been observed that surface runoff occurs only during the most intense rainstorms. This suggests that the dominant hydrological process for water movement downslope is that of subsurface flow. The objectives of this study were to determine the principal hydrological processes occurring on a hillside, and to develop a simple model to simulate these processes.

Firstly the principles underlying our present understanding of hillslope hydrology need to be outlined. Chapter 2 is devoted to doing this. Chapter 3 describes measurements of the water table behaviour and runoff processes found in a humid climate, on a pasture-covered slope with a permeable soil underlain by an impermeable layer at 500 - 700 mm depth. Measurement of soil hydraulic properties is also detailed. Chapter 4 reviews the simulation of hillslope hydrology. Chapter 5 describes a particular model developed to simulate the hillslope hydrological data presented in Chapter 3. Chapter 6 presents and discusses the results obtained using this model. Chapter 7 summarizes the conclusions reached.

CHAPTER 2

HILLSLOPE HYDROLOGICAL PROCESSES

Introduction

The principal components of the hillslope hydrological cycle are illustrated in Figure 2.1 The most common sequence of events is for any rain which has not been intercepted by vegetation to infiltrate into the soil, and then either percolate down to the water table and become groundwater, or return to the atmosphere by evaporation. However, circumstances arise when the processes of overland flow and saturated subsurface flow (throughflow) become major components as contributors to channel flow, over and above the baseflow from groundwater.

Overland flow

When rain falls faster than it can be taken in by the soil, that is, when the infiltration capacity of the soil is less than the rainfall intensity, then the excess flows over the surface, after an initial abstraction due to depression storage. This is the infiltration theory of runoff first proposed by Horton (1933) and has been termed **Hortonian** or **infiltration-excess overland flow**.

In areas where this process is the dominant producer of storm runoff, overland flow is general over large areas of hillside with a sufficiently low infiltration capacity. However, the infiltration capacity is not necessarily constant over a hillside and this led Betson (1964) to use the concept of spatial variability to improve his predictions of the volumes of runoff from small drainage basins. Betson found that in a particular basin the contributing area remained fairly constant

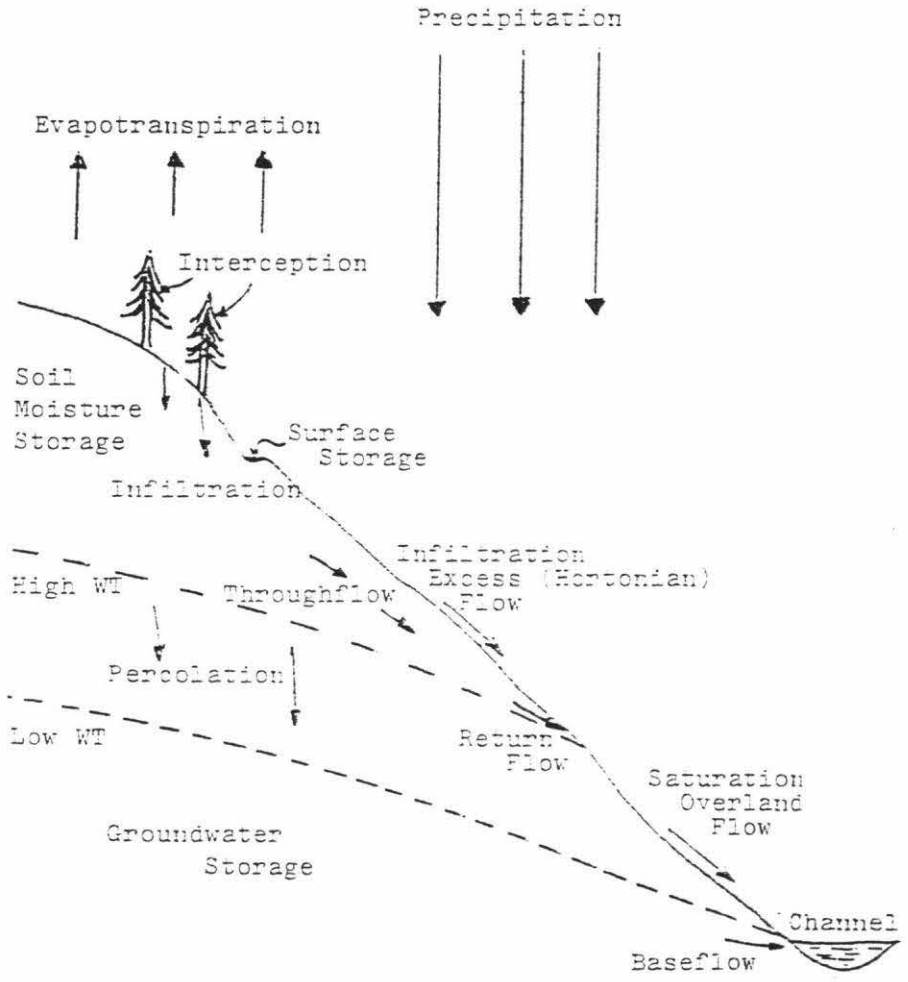

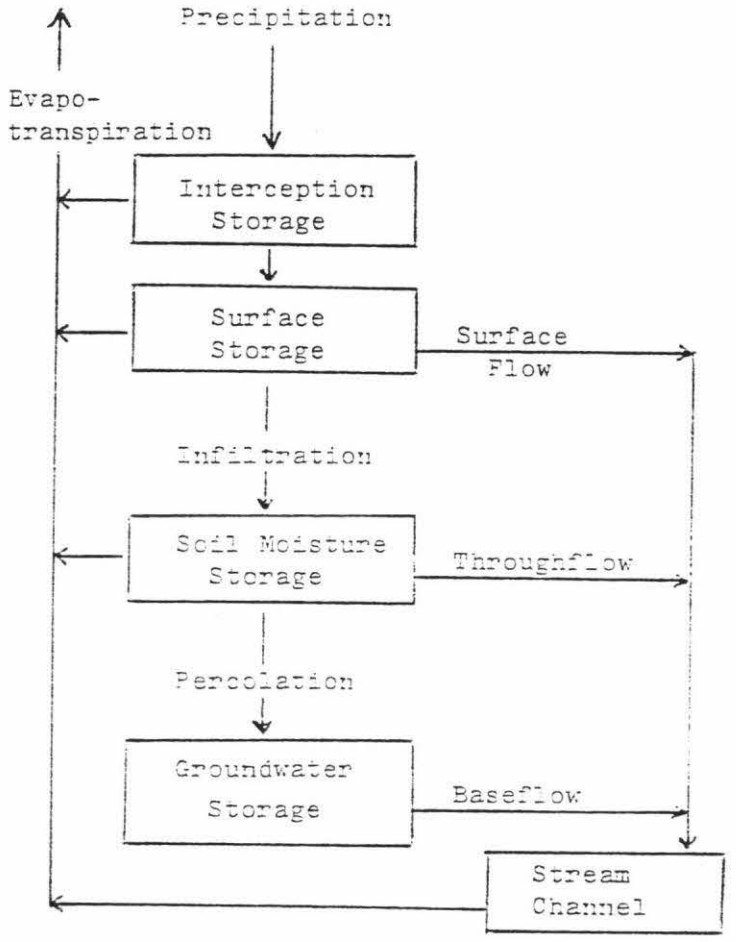

Figure 2.1 The principal components of the hydrological cycle.

throughout and between storms, but it might enlarge during extreme events. He used the term **partial area concept** for his view of the runoff-generating process.

The Horton hypothesis has been found to be most applicable in conditions of sparse vegetation cover and especially in semi-arid and arid climates (Ward, 1984; Dubreuil, 1985). In humid regions where there is appreciable soil and vegetation, and the infiltration capacity of the soil remains high, Hortonian overland flow occurs only during the most extreme storms, or not at all. Then the more dominant runoff generating process is that of **saturation overland flow**. This occurs when the topsoil becomes saturated from both the addition of vertically infiltrating water and the downslope flow of subsurface water (Kirkby and Chorley, 1967). Any further rainfall, even at low intensities, results in overland flow.

Hewlett and Hibbert (1967) explained that streamflow in small upland watersheds is generated in a small saturated area in valley bottoms and hollows:

> "The yielding proportion of the watershed shrinks and expands depending on rainfall amount and antecedent wetness of the soil. When subsurface flow of water from upslope exceeds the capacity of the soil profile to transmit it, the water will come to the surface and the channel length will grow".

This conceptual model is referred to as the **variable source concept**.

A third type of overland flow is **return flow** (Musgrave and Holtan, 1964), which can occur even after rainfall has ceased, where infiltrated water returns to the surface having flowed for a short distance in the upper soil horizon. Return flow is an important process on concave slopes and in areas of flow convergence.

Dunne and Black (1970a; 1970b) made detailed measurements of runoff from a steep, well drained plot containing a deep permeable soil in northeastern Vermont. Over most of the plot in the early part of each

storm, rainfall percolated vertically, displacing water in the soil to the water table. Virtually all the infiltrating water was stored in the soil, raising the level of the water table. Eventually the water table intersected the ground surface in the central hollow at the foot of the concave plot, and outcropped over an expanding area of the hollow as the storm proceeded. Intersection of the ground surface by the water table allowed the return of infiltrated water to the soil surface, where water could move quickly to the channel in larger amounts than could be contributed by the subsurface system. In addition to this return flow, direct precipitation onto the saturated area of the hillside contributed significant amounts of runoff.

As pointed out by Dunne (1978), the area over which return flow and direct precipitation are generated varies seasonally and throughout a storm. This is a major feature of the variable source concept. The fluctuations of the contributing area can be related to topography, soils, antecedent moisture, and rainfall characteristics.

The variable source concept was given a more coherent structure in the mathematical model of Freeze (1972a; 1972b), which describes the generation of runoff from hillsides and small, upland catchments. The model yields numerical solutions to the equations describing saturated-unsaturated subsurface flow, return flow, direct precipitation onto saturated areas and flow in small channels. Freeze investigated runoff production for a range of rainfall duration and intensity, soil conductivity, hillslope shape and soil thickness values. Subsurface stormflow occurred, but because of the impedance of even highly-permeable soils, most of the infiltrating water was stored within the soil, raising the water table to the land surface over an expanding area. The most important control of the volume and peak rate of runoff was found to be saturated hydraulic conductivity. In soils with low conductivities, and especially on concave slopes, hydrographs were dominated by saturation overland flow.

Saturated subsurface flow

The concept of lateral movement of water within the soil is central to contemporary ideas of hillslope hydrology. During the 1940's, Hursh and his co-workers in the Southern Appalachians studied 'subsurface stormflow' which moved at a rate more rapid than the usual groundwater flow. They concluded that a dynamic form of subsurface water may result from the relatively shallow penetration of storm water into the porous upper-soil horizons and its rapid lateral flow downslope (Hursh and Hoover, 1941; Hursh and Fletcher, 1942; Hursh, 1944).

In soils where there is a marked decrease in hydraulic conductivity with depth, and under suitable antecedent moisture and rainfall conditions, saturation may build up from the base of a soil layer within which saturated throughflow may occur downslope. This mechanism has been particularly favoured by forest hydrologists (Hewlett and Hibbert, 1963; Whipkey, 1965) who see the prime requirement as being a shallow soil horizon of high permeability at the surface.

Hewlett and Hibbert (1967) originally envisaged that subsurface flow was by displacement of pre-existing soil water (*viz.* translatory flow) based on the work of Horton and Hawkins (1965). This piston-type flow is most effective in a regime of positive or small negative matric potentials (Harr, 1977). More recently the literature has focussed on the mechanism whereby free water moves preferentially downward through large continuous pores, being partially independent of the hydraulic conditions in the soil matrix (Beven and Germann, 1982; Hammermeister *et al.*, 1982; Mosley, 1982). Such movement can be rapid if it occurs via turbulent, non-Darcy type flow in rodent holes and decayed root channels. Bonell *et al.* (1984) measured near-saturated hydraulic conductivities of 125-2000 mm/hour in the A11 horizon of a clayey soil on the gently sloping forested Keuper formations of Luxembourg.

Other work has emphasized the three-dimensional (Anderson and Burt, 1978; Beven, 1978) as opposed to the two-dimensional (Freeze, 1972b) role of topography, such as hillslope hollows or convergent headwater areas, in

encouraging the convergence of lateral soil-water movement and resulting in subsurface stormflow.

Pilgrim *et al.*, (1978) used radioisotope tracer, flow rate, specific conductance and suspended sediment measurements on a large field plot near Stanford, California to evaluate subsurface runoff. They found that temporarily saturated layers or pathways must occur within the zone above the permanent water table during and immediately after the storm, to allow appreciable lateral movement of subsurface water. Subsurface flow was shown by all the analytical approaches to have a short travel time mainly within macropores. Analysis of the specific conductance data showed that after an initial flushing effect, the subsurface flow was composed almost entirely of new water.

The contribution of lateral soil water movement above a fragipan to streamflow in a small mountainous catchment in central Pennsylvania was determined using a water balance approach by Palkovics and Peterson (1977). Using a grid of 60 observation wells, soil water yield due to perched water table decline was calculated, hydraulic conductivity and the rate of water movement through the soil computed, and the zone contributing to streamflow determined. Results indicated water yield from the soil aquifer explained streamflow, with saturated subsurface flow being the main mechanism. Along a stream length of 400 m throughflow rates of 11 000 - 37 000 litres/day were calculated.

Conclusion

Storm runoff and subsurface storm flow are complex phenomena and encompass a variety of processes. Several of these processes may be operative on a given watershed and it is probable that different processes or groups of processes predominate on different watersheds, particularly under different climatological regimes, geological and pedological settings and vegetative covers. It is also probable that different processes are dominant on a given watershed at various times.

Figure 2.2, adapted from Dunne (1978), shows schematically the relation of the various runoff processes to their major controls.

The next chapter details the water table behaviour and runoff processes found in a humid climate, on a grass-covered slope with a permeable soil underlain by an impermeable layer at 500 - 700 mm depth.

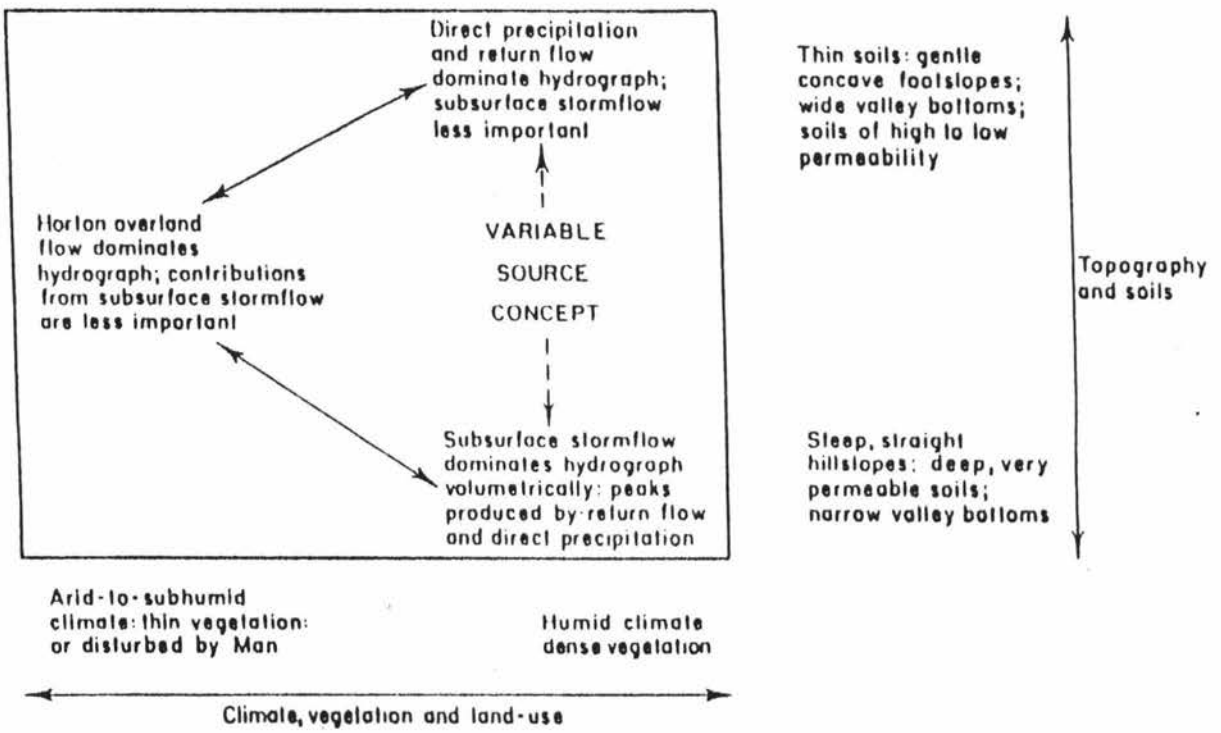

Figure 2.2 Schematic illustration of the occurrence of various runoff processes in relation to their major controls.

CHAPTER 3

MONITORING STORM EVENTS ON A SLOPING TOKOMARU SILT LOAM

Introduction

Over a period of three years the hydrological characteristics of a hillside were determined using large runoff plots and observation wells. During the winter/spring wet seasons the water table behaviour was monitored, and rainfall/runoff data were collected for each storm event. Infiltration and saturated hydraulic conductivity were measured for both undisturbed and severely pugged conditions. The effect of pugging on runoff was also studied.

The experimental site

The research site is located near Massey University at grid reference NZMS260 T24 326871 at an altitude of 60 metres. The average annual rainfall for the location is 955 mm which is spread evenly throughout the year. Variation in the monthly evapotranspiration, however, results in a winter and spring soil water surplus (See Figure 3.1).

The soil type is the Tokomaru silt loam (an Aeric Fragiaqualf) which is characterised by the presence of a densely packed fragipan located at approximately 700 mm below the soil surface (Plate 3.1). This horizon, and to a lesser extent the B horizon above it, impede the movement of percolating soil water, and result in the presence of a perched water table during much of winter and spring.

After a detailed contour survey of the site (Figure 3.2), two nearly identical runoff plots were constructed. Each plot was 16.67 m x 6 m (100 m^2) and had an average slope of 11.5%. The tops and sides were bounded by 150 x 25 mm macrocarpa planks which were buried to 100 mm

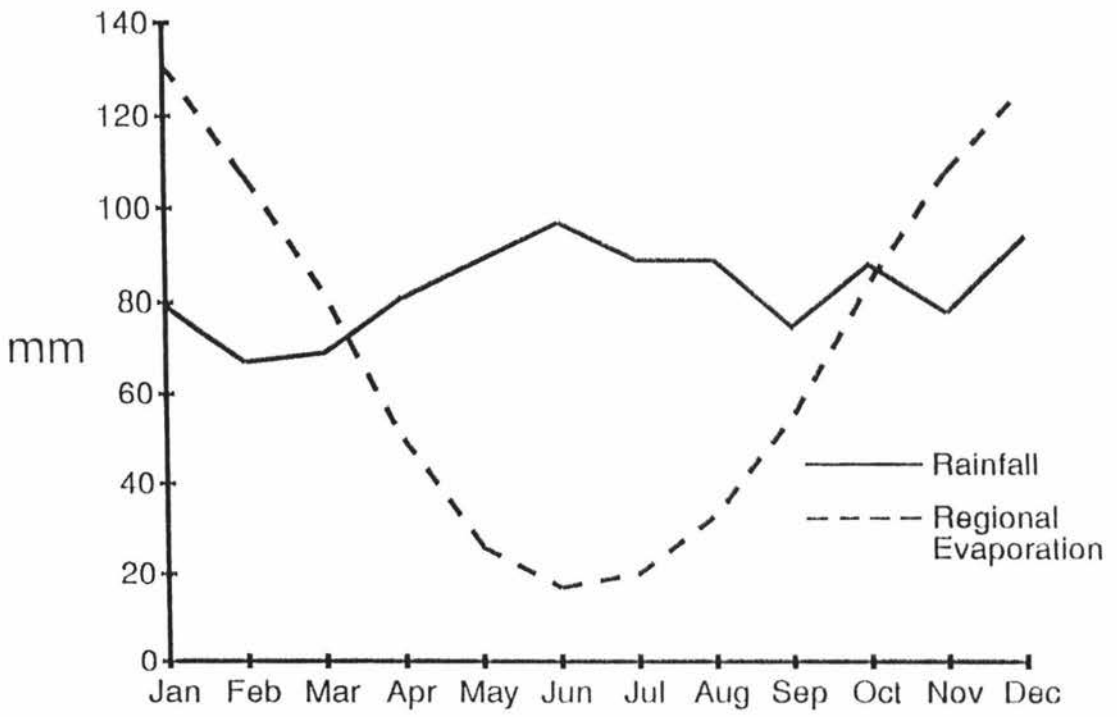

Figure 3.1 Average monthly rainfall and regional evaporation for Palmerston North.

Plate 3.1 Typical soil profile of a Tokomaru silt loam, showing the fragipan at approximately 700 mm and the pseudogley horizon immediately above.

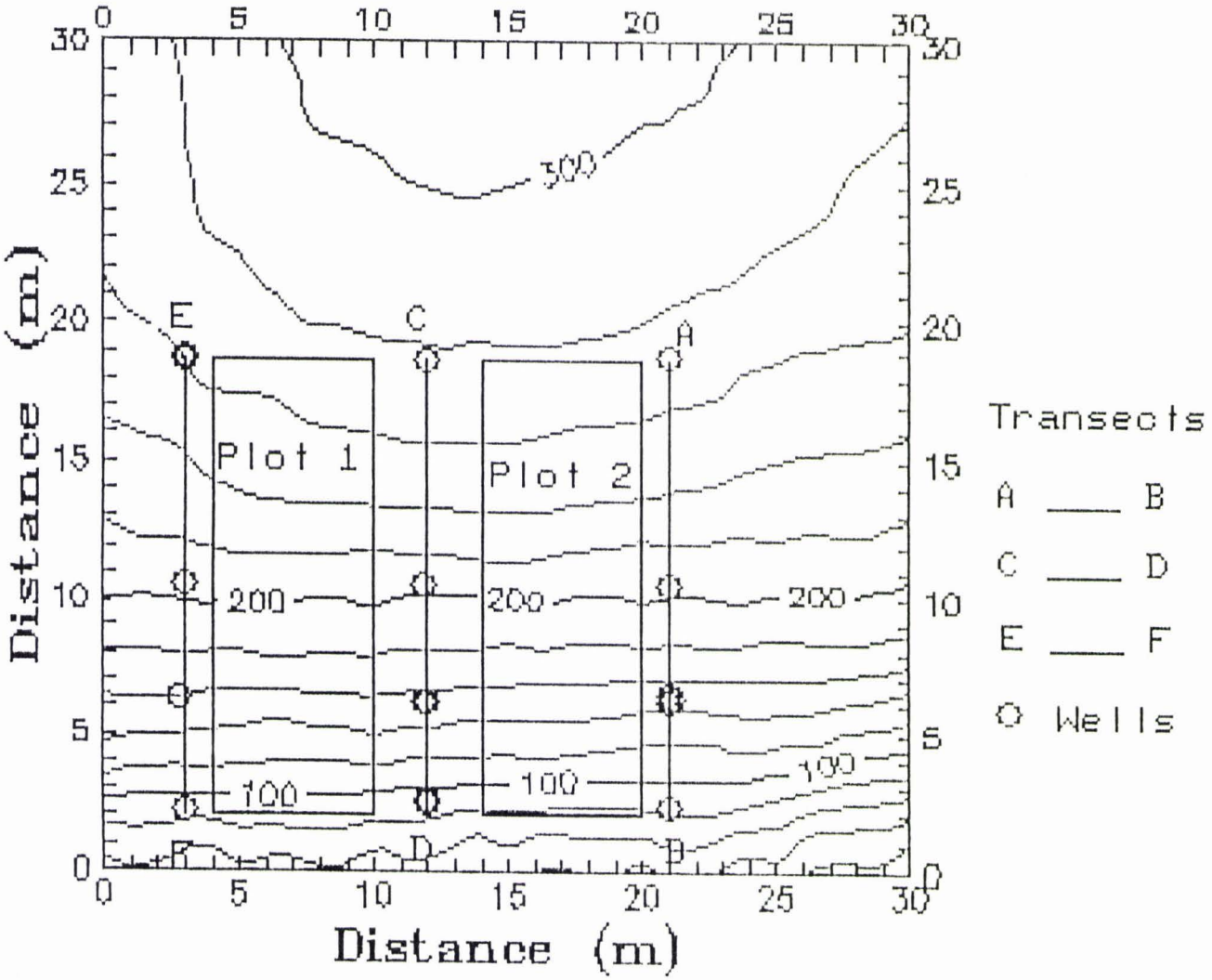

Figure 3.2 Contour plot of the research area showing the locations of the runoff plots and the twelve water table observation wells.

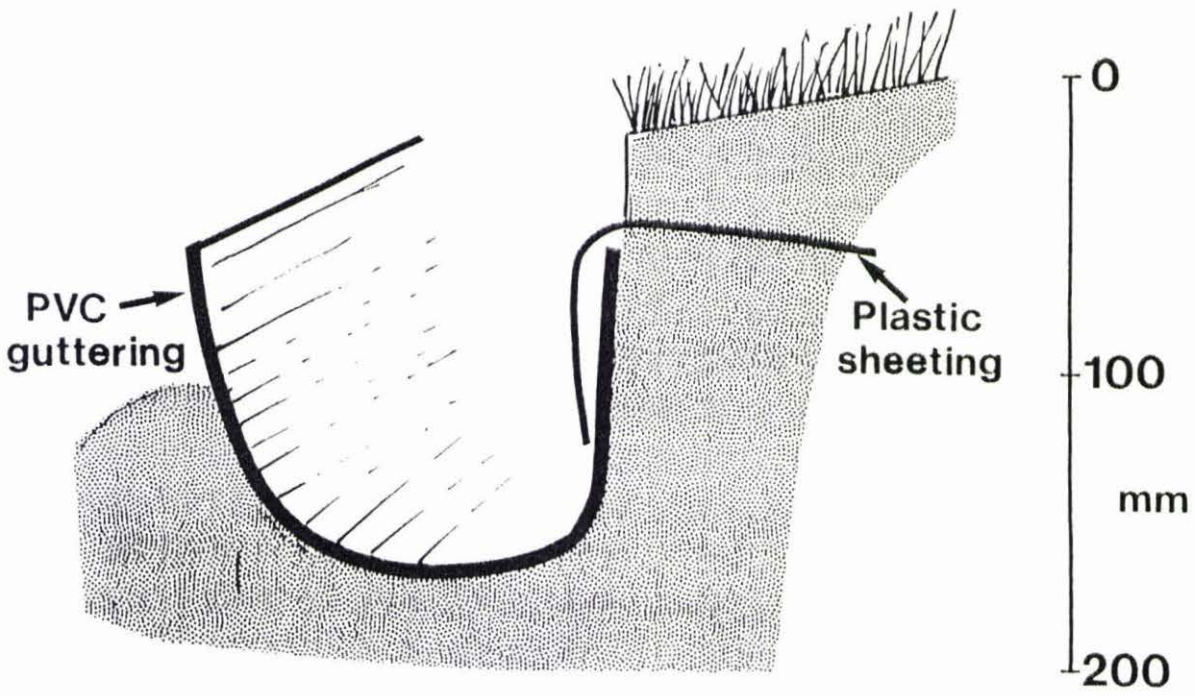

Figure 3.3 Detail of PVC guttering used to collect runoff at the bottom edge of each plot.

Plate 3.2 Hut containing runoff monitoring equipment and cream vats used to collect excess runoff during large storms. The collecting trough at the bottom of Plot 2 is visible at right centre.

Plate 3.3 Stephens Type F water level recorder (right) and the variable potentiometer system (left) used to measure the rate at which runoff filled the 200 l drum.

Plate 3.4 Campbell CR21 micrologger used to record automatically rainfall, runoff and water table depths.

depth. Runoff was collected in PVC guttering (Figure 3.3) and carried in 75 mm alkathene pipes to 200 litre drums housed in a small shed. Once filled, these drums overflowed into 1000 litre cream vats allowing the total runoff to be recorded for larger events (Plate 3.2).

Instrumentation

A system was designed so that rainfall, runoff and water table levels could be recorded automatically on a Campbell CR21 micrologger. Rainfall was measured using a Sierra tipping bucket raingauge, model RG 2501. The tipping bucket mechanism activated a sealed mercury switch that produced a contact closure for each mm of rainfall.

The amount and rate of runoff was measured as the 200 l drums were filled. The water level in each drum was recorded using a float and counterweight system which turned a 100 kΩ linear variable potentiometer. A 2 volt DC excitation voltage output from the micrologger produced a 0-2 volt input depending on the water level.

Water levels were recorded every hour until the beginning of a runoff event when subsequent recordings were made at 10 minute intervals. Backup data were available from a Lambrecht weekly recording raingauge, and two Stephens type F water level recorders for runoff into the 200 l drums (Plates 3.3 and 3.4).

Immediately adjacent to the runoff plots, twelve perforated PVC water table observation wells 50 mm in diameter and 600 mm deep were installed (See Figure 3.2). Water table levels were measured manually with a dip stick. The dip stick contained two wires, an oscillator and headphones, and when the wires reached the water level in the well the electric circuit was completed and an audible tone was heard through the headphones. The water level could then be read from graduations marked on the dip stick.

Surface runoff events during 1983

During the winter and spring of 1983, twenty surface runoff events were recorded. Twelve of these events were relatively minor, each resulting in < 0.5 mm of runoff. Two events produced 4-10 mm (400-1000 litres) of runoff but because of the limitations of the recording equipment, complete hydrographs could not be plotted.

With the runoff being collected in 200 litre drums, the most useful data were obtained from storms which produced 0.5-2 mm of runoff. Three events of this magnitude have been chosen to illustrate the various characteristics of the runoff plots, and their varying responses to changing soil conditions.

The rainfall histogram and runoff hydrographs for the event of August 23, 1983 are shown in Figure 3.4. Total rainfall during the event was 10.3 mm and the surface runoff recorded was 0.72 mm from Plot 1, and 1.8 mm from Plot 2. The percentages of rainfall becoming surface runoff were thus 7% and 18% respectively.

Similar marked differences between the two plots were exhibited in almost every event recorded. The utmost care was taken in selecting the site in the hope of having duplicate plots which produced similar quantities of runoff, and the first few events seemed to indicate that the plots were behaving similarly. However, as the soil became wetter Plot 2 produced consistently more surface runoff than Plot 1.

The reason for this incongruity was probably the closer proximity of Plot 2 to an area of flat land only 5-10 metres from the top of the plots (Figure 3.5).

Once the soil became saturated the natural drainage provided by the hillside resulted in water from the flat area above moving towards the plots as subsurface flow. Apparently some of this subsurface flow exfiltrated within the confines of Plot 2 thus producing the higher quantities of runoff recorded. Further evidence that this flat area was contributing water to Plot 2 was the existence of a very wet area in the

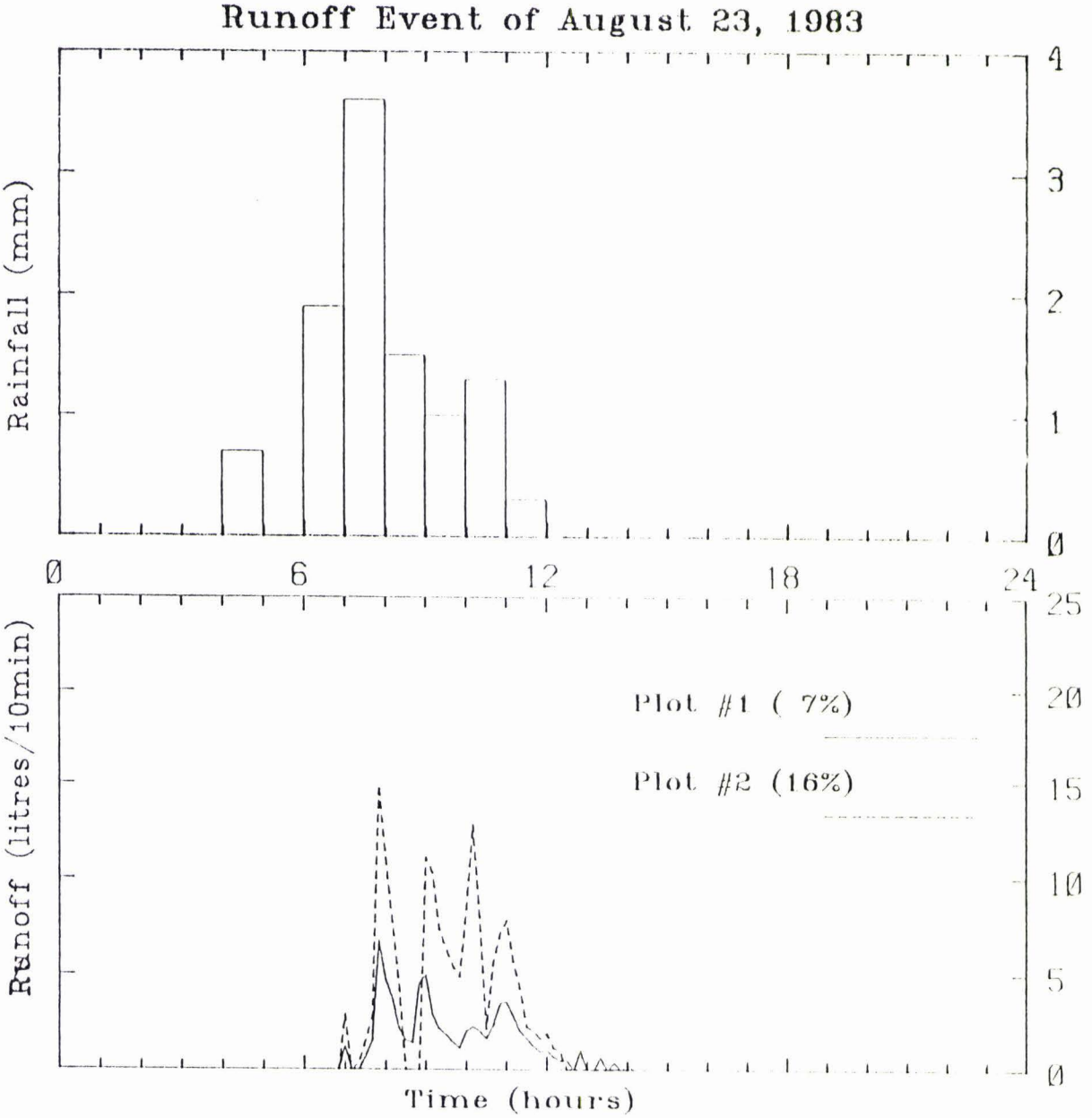

Figure 3.4 Rainfall histogram and runoff hydrograph for the storm event of August 23, 1983. Percentages of rainfall becoming surface runoff are shown in parentheses.

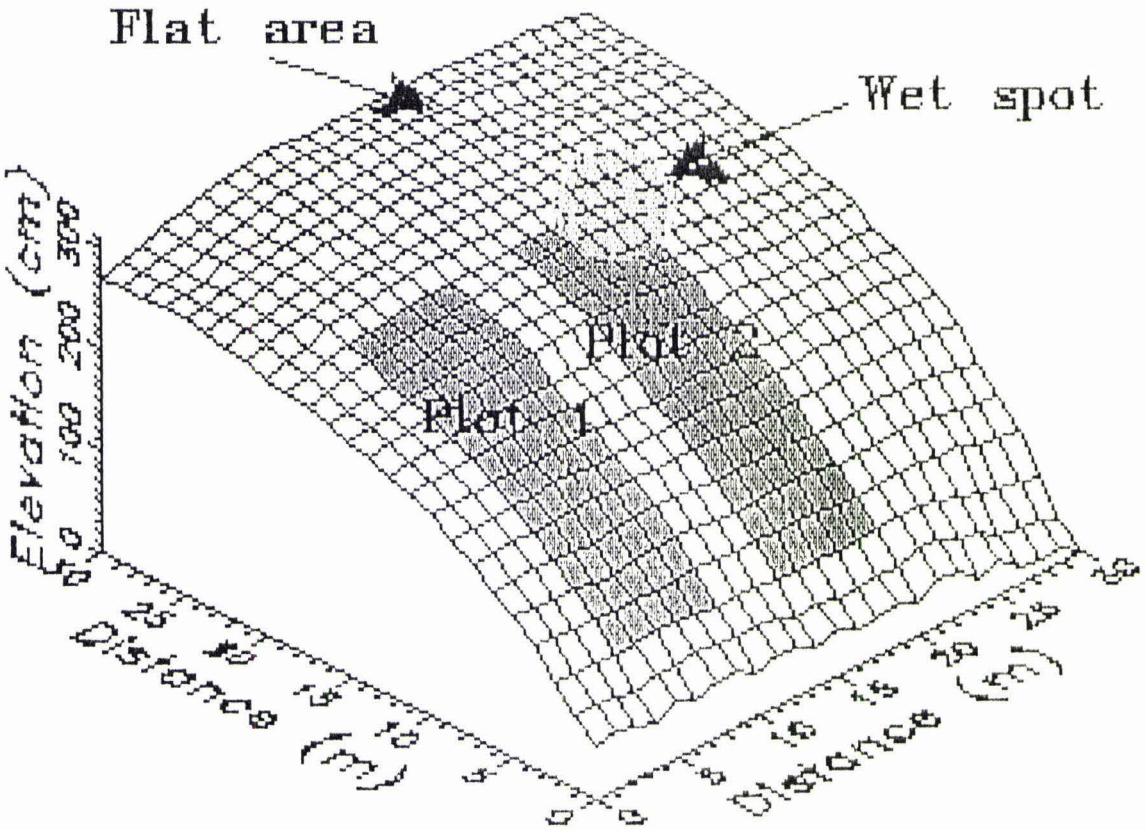

Figure 3.5 Block diagram showing surface characteristics of the research area.

top corner of Plot 2, adjacent to the flat area. No such wet area was in evidence in Plot 1.

The August 23 runoff event is typical of most runoff events occurring at this locality. During the proceeding three and a half days 36.3 mm of rain had fallen, and the soil was at, or very near to saturation just prior to the further 10.3 mm of rain which resulted in the runoff.

The concept of saturation overland flow explains the process occurring in this situation. The impermeable subsurface horizons have restricted the downward movement of water and the drainage provided by lateral subsurface flow does not have the capacity to cope with all the rainfall. At the base of the slope, or where there is a thinning of the soil above the impermeable layer, a saturated wedge may form. As this extends upslope water is brought to the surface and overland flow occurs.

Figure 3.6 shows the rainfall histogram and runoff hydrograph for the event which occurred on September 9, 1983. Once again the topsoil had been brought near to saturation by 20.5 mm of rain falling in the 48 hours preceding the runoff event. A further 4.9 mm of rain in 3 hours produced 0.5 and 1.5 mm of surface runoff from the two plots, with Plot 2 again producing the greater amount.

Measuring saturated hydraulic conductivity (K_S).

The method of Scotter **et al.** (1982) involved sharpened rings, with radii (r) ranging from 0.075 m to 0.204m, being gently driven approximately 10 mm into the soil, just far enough to prevent lateral leakage when water was ponded within them. A ponding depth of approximately 10 mm was used. The infiltration rate as a function of time was found by refilling the rings to a fixed level from a measuring cylinder at suitable time intervals. For this study the time interval was 30 minutes.

Initially three ring radii were used and the resulting mean values of q (flux density) and the standard deviations are shown in Table 3.1

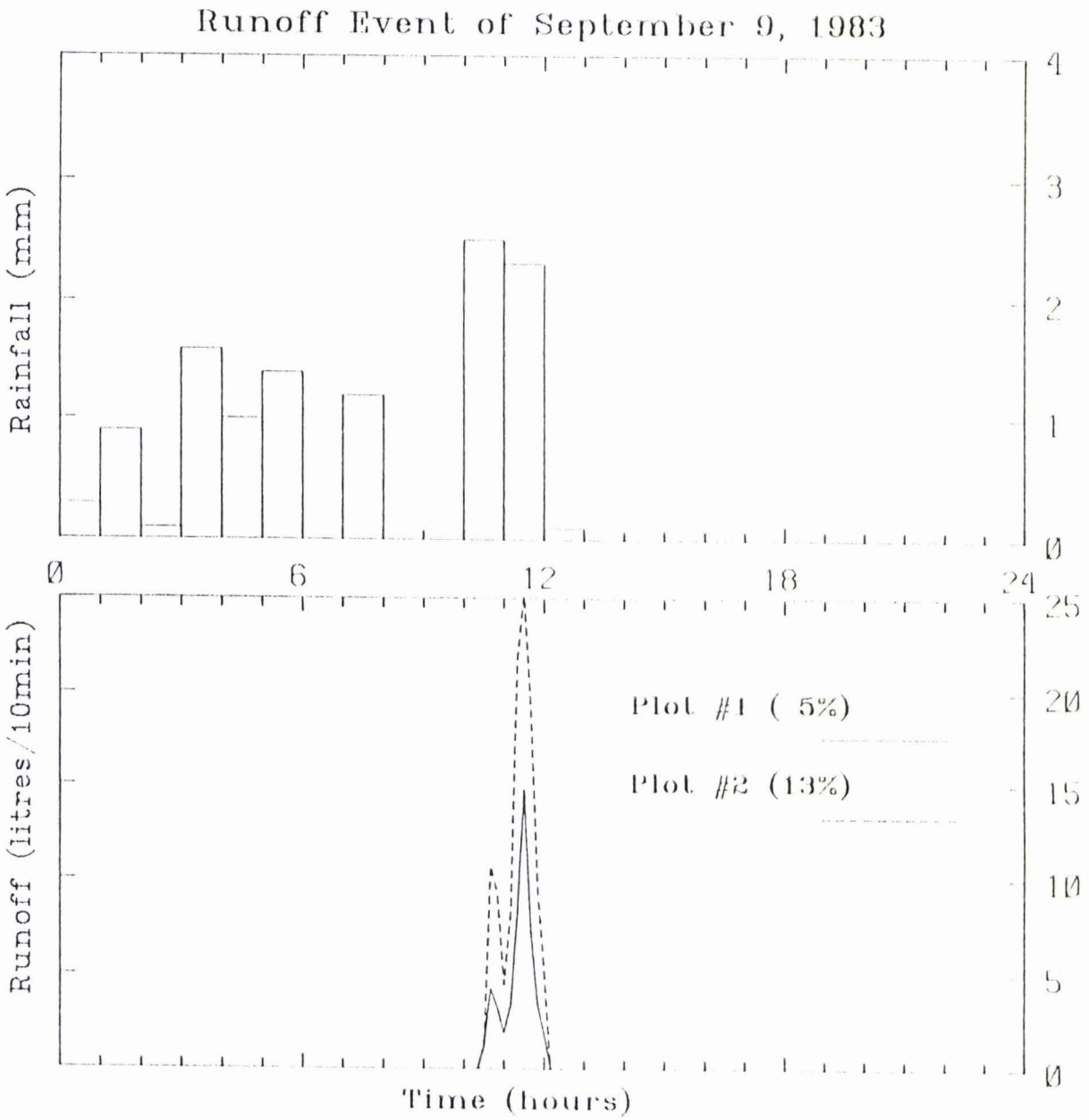

Figure 3.6 Rainfall histogram and runoff hydrograph for the storm event of September 9, 1983. Percentages of rainfall becoming surface runoff are shown in parentheses.

Table 3.1. Infiltration data for runoff plots.

r (m)	n[a]	10^{-6}q (m/s)	10^{-6}s (m/s)
0.204	28	5.5	3.1
0.102	47	4.6	3.1
0.075	25	1.1	1.1

[a] Number of measurements.

Average infiltration rates for the three ring radii were treated as three pairs (I, II, & III) allowing three calculations of saturated hydraulic conductivity (K_s) to be made using

$$K_s = (q_1 r_1 - q_2 r_2) / (r_1 - r_2) \qquad [1]$$

The standard error of K, s(K), was calculated assuming a normal distribution of q by

$$s(K) = [(r_1 s_1)^2/n_1 + (r_2 s_2)^2/n_2]^{1/2} (r_1 - r_2)^{-1} \qquad [2]$$

where s_1 and s_2 are the standard deviations of q_1 and q_2 respectively, and n_1 and n_2 the number of replicate measurements. The resulting values for K_s and s(K) are shown in Table 3.2.

Table 3.2. Saturated hydraulic conductivity data for runoff plots prior to grazing.

Pair	r_1 (m)	r_2	K_s (10^{-6}m/s)	K_s (mm/day)	s(K) (10^{-6}m/s)	s(K) (mm/day)
I	0.204	0.102	6.4	550	1.8	155
II	0.102	0.075	14.4	1245	2.7	230
III	0.204	0.075	8.1	695	1.0	86

The K_s values determined using the twin ring method were considered to be more representative of the 10 - 150 mm soil layer rather than the 0 - 50 mm layer, because the high organic matter content and obvious macroporosity of the surface soil suggested very high permeability.

An alternative technique for measuring K_s in the topmost soil layer was the field-core permeameter method. A 0.037 m radius sharpened cylinder was driven 50 mm into the surface and then dug out. The core and cylinder were stood on a perforated base, water was ponded on the surface, and the flow rate measured when steady flow prevailed so that Darcy's Law could be used to calculate saturated hydraulic conductivity.

The K_s value measured for the surface soil layer using the core method was 1.4×10^{-4} m/s (12000 mm/day) with a standard deviation of 1×10^{-4} m/s. Individual values ranged from 2×10^{-5} to 3.1×10^{-4} m/s (1800 - 27000 mm/day).

This method was also used to determine K_s for the clay-rich layer just above the fragipan. Here values ranged from 6.4×10^{-7} to 2.4×10^{-6} m/s (55 - 210 mm/day) with a standard deviation of 1×10^{-6} m/s (86 mm/day).

The effect of pugging damage on infiltration and runoff

Following four days of persistent rain (50 mm) a mob of 20 sheep was put into Plot 1 for 24 hours on September 11. This action resulted in severe pugging damage (see Plate 3.5), and its effect on the infiltration characteristics and consequently surface runoff generation was quite marked.

Further measurements of K_s using the twin ring method were made less than a week after inflicting the stock treading damage, and again one month later. Only two ring sizes were used for these determinations and the data are shown in Table 3.3.

Table 3.3. Infiltration and saturated hydraulic conductivity data for runoff plots following pugging. (Symbols as in Tables 3.1 and 3.2)

	r (m)	n	q (10^{-6}m/s)	s (10^{-6}m/s)	K_s (10^{-6}m/s)	s(K) (10^{-6}m/s)
Within 1 week	0.204	12	0.38	0.19		
	0.102	18	0.54	0.55	0.22	0.41
After 1 month	0.204	16	7.13	2.77		
	0.102	18	10.12	5.50	3.88	4.2

Two days after pugging the soil a storm event of 7.2 mm over 7 hours resulted in 25% (1.8 mm) of the rainfall becoming surface runoff on Plot 1, and 18% (1.3 mm) of the rainfall becoming surface runoff on Plot 2.

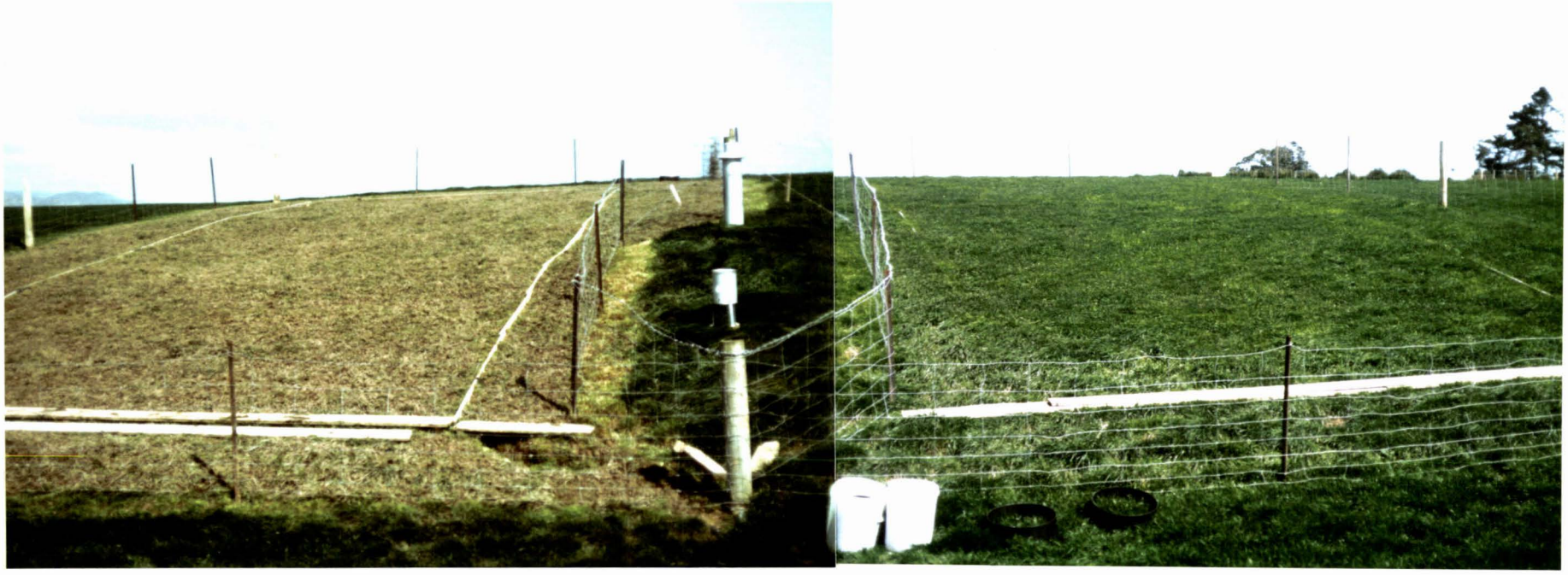

Plate 3.5 The runoff plots on September 13, 1983. Plot 1 (left) shows severe pugging damage.

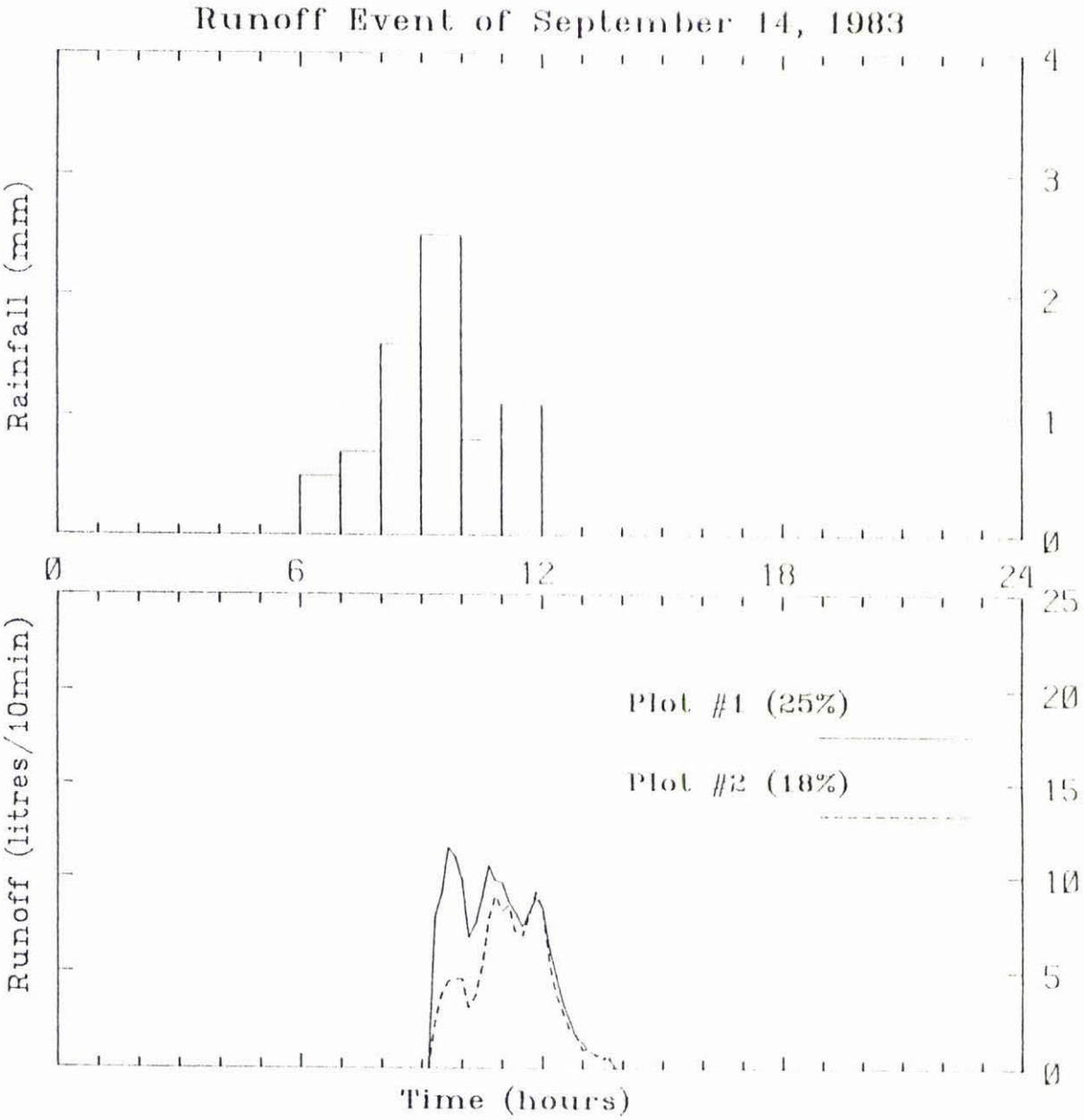

Figure 3.7 Rainfall histogram and runoff hydrograph for the storm event of September 14, 1983. Percentages of rainfall becoming surface runoff are shown in parentheses.

Not only was more runoff being produced from Plot 1, but the shape of the runoff hydrograph as shown in Figure 3.7 also indicates a different process was involved.

In previous events the process of saturation overland flow was responsible for runoff generation. After pugging, the infiltration rate of the surface soil was reduced by an order of magnitude to less than 1 mm/hour. On Plot 1 therefore, Hortonian runoff resulted when the rainfall intensity exceeded the infiltration rate.

While the plot was in a pugged condition an average hydraulic conductivity of 0.8 mm/hour was measured using the twin ring method (see Table 3.3). There were three hours when the rainfall intensity exceeded this rate and the excess rainfall amounted to 2.8 mm. This is comparable with the 1.8 mm of runoff collected, assuming that at least 1 mm of rainfall could be held as surface detention in puddles and hoof-marks on the surface. Further evidence that the runoff from Plot 1 was Hortonian can be seen from the shape of the hydrograph in Figure 3.6. For Plot 1 the time of maximum runoff rate corresponds with the maximum rainfall intensity. In marked contrast, the maximum runoff from Plot 2 occurs in the two hours following the most intense rainfall. This indicates that the process of saturation overland flow is still occurring in that plot.

Recovery after pugging damage

While the pasture was severely trampled and the soil surface sealed for a time, the increase in runoff lead to an increase in soil loss from the damaged area. While the amount of sediment was not measured it was observed qualitatively, and the long-term effects of such erosion could include a reduction in topsoil depth and decreased soil fertility on the hillside, as well as sedimentation problems in farm dams and waterways.

An interesting facet of the pugging experiment was the quick recovery of the pasture. Plate 3.6 shows the condition the plots were in only one month after the pugging damage was inflicted. It is true that this recovery took place in the middle of spring when pasture growth was at a

Plate 3.6 The runoff plots on October 15, 1983. Plot 1 has now recovered from the pugging damage inflicted one month before. Both plots have a healthy pasture sward.

maximum, but it is also worth considering that the damage may not really be as bad as it looks. Much of the grass may only be laid flat and held down in the sticky, muddy surface. Subsequent rain may wash this grass clean and the pasture appears in a much healthier state. Horne (1985) gives more detail on treading damage, and subsequent pasture recovery on a flat site.

An improvement in the K_s value of the surface soil was also noted after one month's recovery. It increased from 0.8 mm/hour to 14 mm/hour, a change of more than an order of magnitude, to a rate which could comfortably cope with most rainstorms.

Water table decline

During the last week of June and the first two weeks of July, 1984 nearly 85 mm of rain fell. The heaviest falls were on July 12 (17.2 mm) and July 14 (13.5 mm), and on both occasions almost 2 mm of surface runoff was recorded from Plot 2, while Plot 1 produced less than 0.5 mm. A further 3.6 mm precipitation over 6 hours on July 16 brought the water table to the surface but produced no recorded surface runoff.

Apart from a few light showers on July 17, the following six days were fine, and the decline of the water table was monitored manually in 12 wells along the transects whose locations are illustrated in Figure 3.2

Water table depths were measured immediately following the cessation of rain at 1100 hours on July 16 (Time 0). Further recordings were made 5 hours, 26 hours and 101 hours after time 0. Water table decline along each of the transects is illustrated in Figure 3.8.

The behaviour of the water table along transect A-B is consistent with the observation that near A, a very wet area existed. Apparently water moved from the flat hilltop area described earlier, through the soil in the vicinity of the top corner of Plot 2. This resulted in the water table there remaining within 120 mm of the surface as much as a day after rain had stopped.

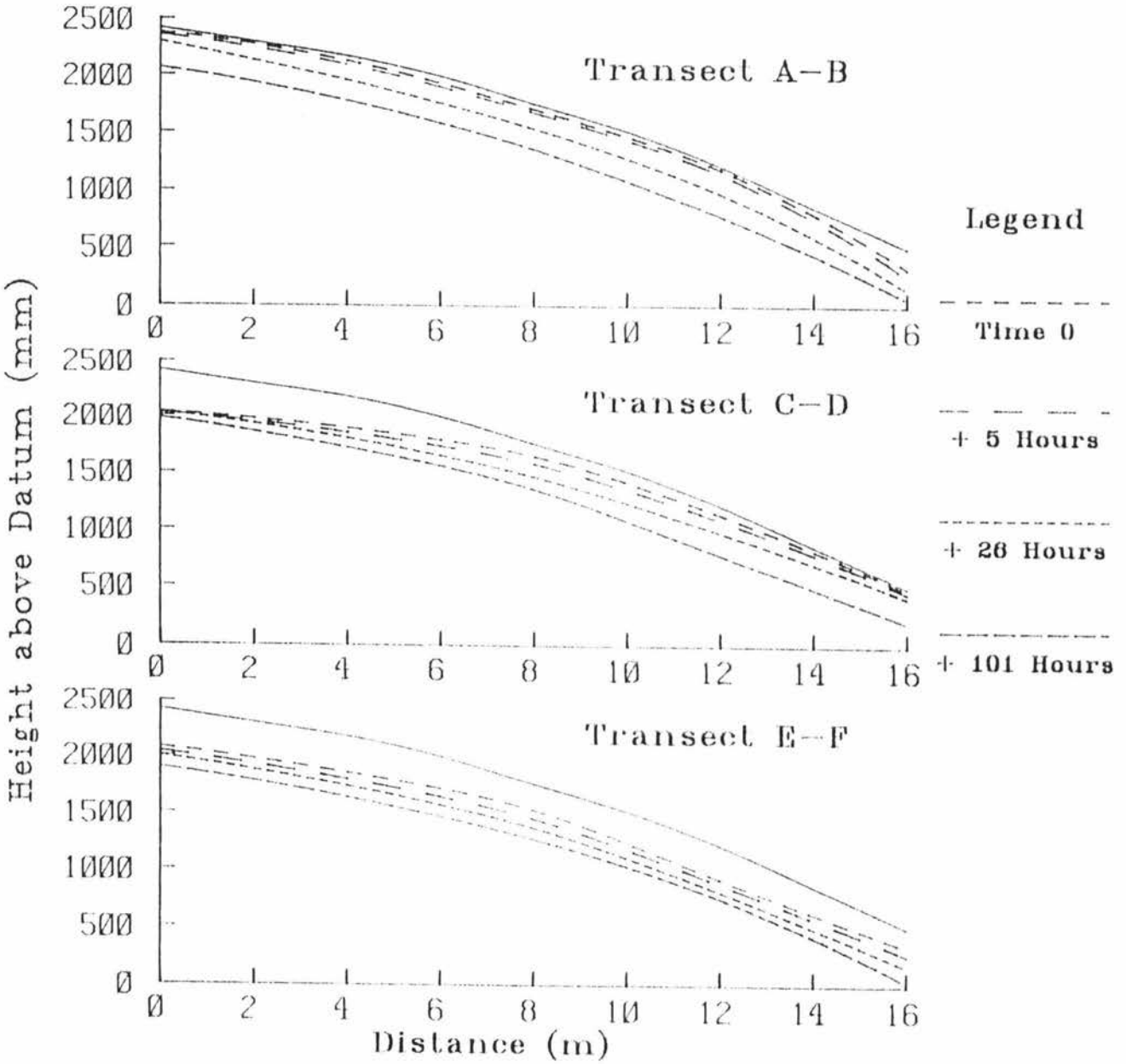

Figure 3.8 Water table decline, measured along three transects adjacent to the runoff plots, following the storm events of July 12-16, 1984.

At the lower end of transect A-B the water table remains below 180 mm depth. Perhaps the most likely explanation for this is the variability of the permeability within the soil. Near B there seems to be a higher permeability in the surface horizons than at other points along transect A-B. With the subsurface water passing through this point more quickly, the water table is correspondingly lower.

After 101 hours drainage, the water table is nearing the much less permeable pseudo gley horizon at all points along the transect, and hence the depth to the phreatic surface is more constant at around 400-450 mm.

The water table behaviour along transect C-D is more easily explained; in fact it is as one would expect the water table on a hillside to decline. Water from uphill moves through the soil, but if the drainage at the base of the slope is unable to discharge water at the rate which it arrives, then the water table at the lower part of the slope remains high. Eventually this 'saturated wedge' diminishes and once again the water table falls to a similar depth along the length of the transect.

Transect E-F shows a lower water table than along the other two transects, especially during the first few hours following the end of the rainfall. Once again the lower water table probably reflects a higher permeability in the soil, and so a greater ability of the soil to conduct water downslope within the top 300 mm. This greater lateral subsurface flow may also explain in part why Plot 1 produces much less surface runoff than Plot 2.

Conclusion

The plot studies have shown that for the conditions encountered at the study site - mostly low intensity rainfall, well vegetated slopes, permeable soils underlain by a fragipan - the most common runoff process is that known as saturation overland flow. However, if the surface is damaged by stock treading, the Hortonian process of runoff generation may occur as the infiltration capacity of the surface soil is reduced substantially.

CHAPTER 4

THE PHILOSOPHY OF MODELLING AND SIMULATION

Introduction

The role of agricultural and environmental research is "to generate basic knowledge of the complex system to be managed and to apply such knowledge toward the optimization of all controllable factors so as to achieve a higher level of production on a sustainable basis without damaging the environment. Some of the fundamental problems of agricultural and environmental research are how to obtain knowledge of specific processes within a complex system of interacting and interdependent phenomena, and then how to reintegrate such knowledge so as to obtain a comprehensive understanding of the way the system as a whole operates" (Hillel, 1977).

In recent years, mathematical modelling and simulation techniques, relying on the use of high-speed computers, have been developed for the purpose of providing a comprehensive quantitative description of the behaviour of dynamic systems. In the process of designing, operating, and attempting to validate a simulation model, we gain insight into the workings of the complex natural system and develop criteria for predicting its future behaviour under varying conditions.

Definitions

The phrase 'modelling and simulation' designates the complex of activities associated with constructing models of real world systems and simulating them on a computer. When we engage in modelling and simulation, we are concerned not only with the elements themselves but also with establishing certain relationships among them. In particular,

modelling deals primarily with the relationships between real systems and models; simulation refers primarily to the relationships between computers and models (Zeigler, 1976).

A **real system** is some part of the real world which is of interest. It refers to nothing more or less than a source of observable data. The important characteristic is the identification of a segment of reality and the distinguishing of it from the rest, permitting measurements and other observations to be made on it. The observable, descriptive variables (thought to be significant for the understanding, and/or control of the system) can be classified as input or output variables. Input variables can be thought of as causes of a system's behaviour and output variables as effects. The set of all possible experimentally obtainable input-output pairs is called the input-output behaviour of the real system and this constitutes all that can be directly known about the real system.

A **model** is basically a set of instructions for generating behavioural data. A base model is capable of accounting for all the input-output behaviour of a real system. In any realistic modelling and simulation area, the base model description (a hypothetical complete explanation) can never be fully known. However, by specifying an experimental frame it is possible to construct a relatively simple model by lumping together components and simplifying interactions. The experimental frame characterizes a limited set of circumstances under which the real system is to be observed or experimented with; it puts constraints on the possible observation of the real system. A model, then, is a simplified, and hence more readily definable and more easily tractable, version of reality.

A **computer** is a computational device capable of generating behavioural data when supplied with suitably encoded model instructions. It performs the step by step simulation process whereby input-output segments are worked out from one simulated time instant to the next. The speed and efficiency of modern electronic computers has made possible the consideration of models of complexity undreamed of in prior eras, nevertheless there still exist limits to the resources available both of

the computer and the modeller. The primary constraints to most model building efforts are time, space and money. A model whose complexity exceeds the limits imposed by the project budget is useless even if it is valid in some desired experimental frame.

The **modelling relation** concerns the validity of a model, that is, how well a model represents the real system. Zeigler (1976) states that there are three degrees of strength for model validity. Firstly, a model may be **replicatively valid** if it matches data already acquired from the real system. Stronger than this is the condition in which the model is predictively valid, that is, when it can match data before they are acquired from the real system (or at least before they are seen by the model). A third, stronger level of validity concerns the relation between the structure of the model - what makes it do what it does - and the internal workings of the real system. A model is structurally valid if it not only reproduces the observed real system behaviour, but truly reflects the way in which the real system operates to produce this behaviour.

The **simulation relation** concerns the faithfulness with which the computer carries out the instructions intended by the model. This is often referred to as the correctness of the program, and is reflected in the accuracy of the data produced by the computer. Oren (1979) has explained experimentation as "controlled observation" which can be done either with the real system or with one of its models; simulation is "experimentation with models".

There are several reasons for substituting a model for a real system. Experimenting with the real system may be costly and time consuming, or even impossible in many situations. In addition, computer simulation experiments are completely repeatable and non destructive. Finally, data acquired from computer simulation are often easier to interpret and to reduce to statistical and graphical summaries, especially considering the facilities provided by many of the specialized simulation languages (e.g. CSMP, GASP) for this purpose.

As stated by Hillel (1975) "the systematic results of computer simulation will never obviate experimentation with the real system, which is required for supplying parameters, calibrating, and testing the simulation, but such results can help economize experimentation and increase its efficiency by guiding it to where it is needed most". The value of a simulation model is proportional to the degree to which it helps us to understand and manage reality. A model which is too simplistic will probably be too unrealistic. One which is too complex may also be unwieldy or incomprehensible.

Mathematical models

Clarke (1973) has described mathematical models as those in which "the behaviour of the system is represented by a set of equations, perhaps together with logical statements, expressing relationships between variables" (measurable, time-variant characteristics) "and parameters" (time-invariant characteristics). Such models may be classified as **conceptual** or **empirical** according to whether the relationship is, or is not, suggested by consideration of the physical processes acting upon the input variables to produce the output variables. The distinction is almost entirely artificial; Darcy's Law, for example, is a matter of observation, and hence is empirical by strict definition (cf. the Oxford Dictionary: empiric (al) = based, acting, on observation and experiment, not on theory), a point recognised by Mandelbrot (1970).

Another common distinction between mathematical models is whether they are **deterministic** or **stochastic**. According to Chow (1964) "if the chance of occurrence of the variables involved in such a process is ignored and the model is considered to follow a definite law of certainty but not any law of probability, the process and its model are described as deterministic. On the other hand, if the chance of occurrence of the variables is taken into consideration and the concept of probability is introduced in formulating the model, the process and its model are described as stochastic or probabilistic".

In a deterministic model current state and current input, if any, uniquely determine the next values of state variables. A stochastic model has at least one random variable and therefore, at a given instant in time, the next state of the model is not uniquely determined.

Stochastic and deterministic methods in modelling should be seen as complimentary rather than as alternatives. A set of dynamic equations that describe the causal behaviour of a system under certain conditions, may be arrived at by coupling the basic principles of conservation of mass, momentum and energy to the constitutive equations for an "ideal" material to ensure mathematical solution. However Kisiel (1971) points out that "inherent in these dynamic equations is a limited capability for predicting or localizing events in space-time because of uncertainties in initial conditions, model, and parameters and because of the stochastic character of forcing functions in space and time".

Finally, a mathematical model may be **lumped** or **distributed** depending on whether or not spatial variability in input variables or model parameters is considered. A lumped model takes no account of the spatial distribution in the input variables, nor of the spatial variation in parameters characterizing the physical processes acting upon input.

A distributed model attempts to incorporate data on the areal distribution of parameter variations and input variables with computational algorithms to evaluate the influence of this distribution on the simulated behaviour.

Becker (1974), with reference to hydrological models, distinguished two classes of distributed model. A probability-distributed model describes spatial variability without reference to the geometrical configuration of the points in the network at which an input variable such as rainfall is measured, or for which a model parameter is to be measured or estimated. A geometrically-distributed model, on the other hand, expresses spatial variability in terms of the orientation of the network points, one to another, and their distances apart.

Communication

One of the most important aspects of modelling, and one of the least appreciated, is communication. In the words of Zeigler (1976) "the long-term contribution of any modelling effort lies in the benefits it affords, either by direct use or by guidance for further development, to science and industry". This requires that the modeller be able to communicate to others what he or she has accomplished. These days, programming language designers are emphasizing **readability** (the ability of a language to be understood) and **annotatability** (the facility with which program instructions and segments can be isolated, explained and commented on).

RAINFALL-RUNOFF MODELS

Introduction

"The hydrology of surface waters is characterized by the multiplicity of prediction formulas that have been devised to facilitate the prediction of runoff rates and volumes". This observation by Merva *et al.* (1969) is just as relevant today, and it applies equally well to most aspects of hydrologic modelling.

One reason for the large number of rainfall-runoff models that have been developed involves advancing technology. Prior to the relatively recent development of electronic computers, the need for manual computation required so many simplifying assumptions that many diverse approaches could yield rational results (Betson and Ardis, 1978).

A more basic reason for the plethora of models lies in the fact that models are, at best nature-imitating. The typical heterogeneity in the soils on a hill slope, for example, introduces so much variability into the modelling problem that exact process modelling becomes an impossibility. The development of a hydrologic model involves a compromise between those processes and detail the modeller would like to

incorporate, and those for which he or she can obtain data and reasonably expect to include in the model.

A continuing growth in the number of models is assured because of the varying degree of detail required, the amount of data available, the number of simplifying assumptions made and the many different ultimate applications.

Infiltration and the hydrological cycle

Infiltration is the key process determining the fate of precipitation, converting it to either runoff or additions to soil moisture storage. However, the infiltration process and other hydrological processes are interrelated through a common dependence on soil moisture conditions. Thus, simulation of infiltration cannot be achieved in isolation; it is best achieved in a model incorporating all the relevant processes. One-dimensional vertical infiltration is the commonest form of the process, and this needs to be modelled for computations of the soil water balance and for predictions of catchment runoff (Dunin, 1976).

As discussed in Chapter 1, surface ponding and overland flow result when the rainfall intensity exceeds the infiltration rate. Such a mechanism, proposed originally by Horton (1933), has won universal acceptance as one of the means of runoff generation. The initial development of Horton's mechanism contained an assumption for uniform infiltration with simultaneous surface saturation occurring throughout the slope. The resultant overland flow was then taken as the dominant component of streamflow.

The partial area concept of runoff generation (Betson, 1964) denies the uniform entry property of the surface: it suggests that the rapid response in the hydrograph is attributable to areas of low infiltration.

Interaction between the infiltration process and soil moisture conditions provides an insight into the variable occurrence of rainfall excess during rain events. Except where water repellency occurs, the antecedent

moisture increases, so the probability of overland flow increases. Thus, in catchment systems the distribution of soil moisture, both spatial and temporal, systematically affects the potential for surface runoff. Topography induces a concentration of water in the lower regions of catchments and causes a high moisture content in those areas (Zaslavsky and Rogowski, 1969), thereby enhancing the possibility of partial area contributions to runoff. Seasonal factors may alter the spatial distribution of soil moisture, so modifying the extent of the contributing area with time.

Through their development of the Stanford Watershed model, Crawford and Linsley (1962; 1966) provided the pioneering effort to make watershed modelling practical for general use. They represented each process by an equation or series of equations containing parameters which vary in value for different watersheds, and for which specific values are read in the input data. The concept was to express each equation in a general form which would apply to all watersheds. The model is applied by using a set of parameter values found through trial and error, to provide acceptable matching of simulated to recorded flows or measured moisture storages.

The trial-and-error calibration requires ingenuity, familiarity with the model, and some understanding of the sensitivity of simulated flows to specific adjustments. However, the selection of a final set of values for the parameters is fundamentally subjective, and this results in the problem of variations in estimates among individual users. Another problem is that because of measurement errors in rainfall and evapotranspiration data, and recorded flows, one can never exactly match simulated to recorded flows. Also several combinations of parameters can produce nearly equally good results (James, 1972).

The Stanford model is a continuous accounting model, in the sense that the location of the water within the system is continuously known. It operates on a 15 minute cycle, i.e. adjustments in the location of water in the system are made each 15 minutes. The model consists of storage units, with flow between the units prescribed by relationships which approximate the physical phenomena.

The infiltration process in the model is expressed as a cumulative frequency distribution of infiltration potential, whose values at a given point may vary with the median soil water content of the catchment. Dunin (1976) points out that "such features in the infiltration function facilitate the simulation of the partial area contributions to runoff and the increase in infiltration rates with increasing intensity, common field phenomena but ones not necessarily reproduced by all infiltration functions."

This assumption that infiltration capacity has a linear cumulative frequency distribution implies that in a catchment there will be a range of infiltration capacities from zero to some maximum value (a parameter). As the rainfall increases, the infiltration capacity of increasingly larger areas will be exceeded, and surface ponding and runoff will become more widespread.

The U.S. Department of Agriculture Hydrography Laboratory Model USDAHL-74 (Holtan *et al.*, 1975) is probably one of the more rational of the continuous-flow models available. Soils in each watershed are grouped by land capability classes to form hydrologic response zones for computing infiltration, evapotranspiration, and overland flow.

The three zones, upland, hillslope, and bottom land, typically are each likely to have characteristics that distinguish their hydrologic response from other zones within a watershed in several ways: (1) elevation affects the water balance of the site through its influence on evapotranspiration and drainage, (2) soil physical properties affect the disposition of rainfall, and (3) distance from the stream channel is an important factor in flood routing (England and Onstad, 1968).

Infiltration in the USDAHL-74 Model is determined by an exhaustion phenomenon equation presented by Holtan (1965):

$$i = aS_a^{1.4} + i_c \qquad [3]$$

where i = infiltration rate (mm/hour)

a = infiltration capacity (mm/hour per mm of available storage)

S_a = available storage in the surface layer (mm)

i_c = constant infiltration rate after prolonged wetting (mm/hour)

Holtan and Lopez (1971) presented estimates of "a" ranging from 0.1 to 1.0 for various types of vegetation. These were evaluated at plant maturity as the percentage of the ground surface area occupied by plant stems or root crowns. Stems and root crowns were assumed to reflect the fraction of porosity in the top soil layer that is surface-connected by mature plant roots to form conduits for air or water.

Estimates of i_c were obtained from the SCS Handbook (USDA Soil Conservation Service, 1972) wherein soils are grouped into four hydrologic classes according to their rate of water intake after prolonged wetting. Musgrave (1955) gave the associated rates of i_c in mm per hour as follows:

A = 11.4-7.6, B = 7.6-3.8, C = 3.8-1.3 and D = 1.3-0

Infiltration and rainfall excess are computed for each soil zone by comparing observed rainfall to the infiltration capacities computed in Equation [1]. Rainfall in excess of infiltration is then routed across each soil zone and cascaded downslope, subject to further infiltration, across designated subsequent soil zones en route to the channel.

Huggins and Monke (1966; 1968) developed a general mathematical model to simulate surface runoff from small watersheds, which avoided the use of lumped parameters by delineating the watershed as a grid of small, independent elements. Each element had to be of sufficiently small size

that all hydrologically significant parameters, e.g. slope steepness, vegetation, rainfall and infiltration rates etc., were uniform within its boundaries. Basically, their analysis required the development of a runoff hydrograph for each elemental area and the integration of these responses over the entire watershed.

An approach that appears capable of identifying and quantifying the actual source areas of runoff on a hillslope was described by Engman and Rogowski (1974). Their storm hydrograph model utilizes a physically based infiltration capacity distribution for computation of rainfall excess, and it incorporates two stages of kinematic routing. In the first stage the rainfall excess is routed over a flow plane to become the lateral inflow hydrograph for the second or channel phase. The overland flow plane expands upslope as the infiltration capacity is exceeded, the size of contributing area and the length of the flow plane being calculated from infiltration curves.

The general theory of infiltration was summarized by Philip (1969) and his two parameter infiltration equation was the preferred means of modelling the process in this instance. The Philip equation for infiltration from a ponded surface is:

$$i = St^{-\frac{1}{2}} + a \qquad [4]$$

where i = infiltration rate $[LT^{-1}]$

S = sorptivity $[LT^{-\frac{1}{2}}]$

t = time

a = a fitted parameter related to the hydraulic conductivity $[LT^{-1}]$

Sorptivity values were computed from Parlange's (1972) approximation

$$S = \left[2 \int_{\theta_i}^{\theta_1} (\theta - \theta_i)\ D\ d\theta\right]^{1/2} \qquad [5]$$

where θ_1 = water content at the soil surface

θ_i = initial soil water content

D = Soil water diffusivity defined as the product of the hydraulic conductivity K and the slope of the moisture characteristic curve $\psi(\theta)$

i.e. $$D(\theta) = K(\theta)\ (d\psi/d\theta) \qquad [6]$$

Hydraulic conductivity as a function of soil water content, and moisture characteristic curves were computed from models proposed by Rogowski (1971, 1972).

The partial differential equation for vertical, one-phase unsaturated flow of water in soils was used as a mathematical model governing infiltration in the surface runoff models of Smith and Woolhiser (1971), Smith and Chery (1973) and Rovey *et al.*, (1977). This equation, often referred to as Richards' equation after Richards (1931), can be written

$$f \frac{\partial S_w}{\partial t} = K_s \frac{\partial}{\partial z} \left(k_r \frac{\partial \psi}{\partial z}\right) - K_s \frac{\partial k_r}{\partial z} \qquad [7]$$

where f = porosity

S_w = relative saturation

K_s = saturated hydraulic conductivity

k_r = relative hydraulic conductivity

ψ = soil capillary potential

z = distance below the surface.

The solution of this non-linear differential equation requires a knowledge of the functional relationships among ψ, S_w and k_r and the values of f and K_s for a particular soil. Smith and Woolhiser (1971)

used an implicit finite difference method to solve Richards' equation for a wide variety of rainfall rates and initial conditions. These results were summarized by parametric relations reported by Smith (1972).

Under the boundary conditions used, $K_s.k_r(0)$ is the asymptotic infiltration rate (i_∞) as $t \rightarrow \infty$. The time at which $\psi(0,t) \rightarrow 0$ marks the beginning of runoff and decay of the infiltration rate. This time is called time to ponding, t_p. For $t > t_p$ the best fit curve was found to be:

$$i = i_\infty + a(t - t_o)^{-b} \qquad [8]$$

where a, t_o and b are parameters unique to a given soil initial saturation and rainfall rate.

Another model which developed the variable source area concept was described by Hewlett and Troendle (1975). To secure a variable source, a rule for iteratively subdividing the watershed into segments, and segments into increments was devised. Each segment is divided into increments beginning with narrow ones along the stream and ending with wider ones along the divides (Figure 4.1). A set of functions generates a mean conductivity value for each element at each iteration from known relations between moisture content and hydraulic conductivity.

To estimate the water flux between elements a finite difference form of the Darcy-Buckingham equation is used. This requires data on the hydraulic head at the centre points of the elements, the hydraulic conductivity, the horizontal distance of the centre points from the datum at the perennial stream channel, and the surface area of the two elements involved.

An approximate method is used for estimating $K(\theta)$ based on a measured moisture release curve $\psi(\theta)$. The latter is expressed by a curve of the form (Hillel, 1971):

$$\psi(\theta) = a\theta^b \qquad [9]$$

where a and b are empirical constants, and the conductivity values estimated from Green and Corey (1971) had the following form:

$$K(\theta) = ae^b \qquad [10]$$

where a and b are empirical constants. When the flux for each element has been computed for the 15-minute interval, all element moisture contents are updated. If the lower elements cannot accept the flow, excess water remains in the source element until it is saturated. If the gravity gradient apparently induces flow into a saturated element, water collects in the element above and/or flows out onto the surface by exfiltration.

When any number of surface elements within the variable source area become saturated, the "channel surface" expands to the exfiltration line and redissection of the remaining slope occurs (see Figure 4.1). The program is thereby always most sensitive at the variable source perimeter.

An alternative approach to modelling the rainfall-runoff processes on a hillslope is that of Freeze (1980). He proposed that a stochastic-conceptual mathematical model of the hydrologic processes be used to investigate the influence of the spatial stochastic properties of the hillslope parameters on the statistical properties of the resulting runoff events.

The mathematical model is conceptual, because it uses a set of physically based equations to route rainfall events through a hillslope. It involves spatially distributed calculations of infiltration rates, moisture contents, and water table positions using a set of parametric

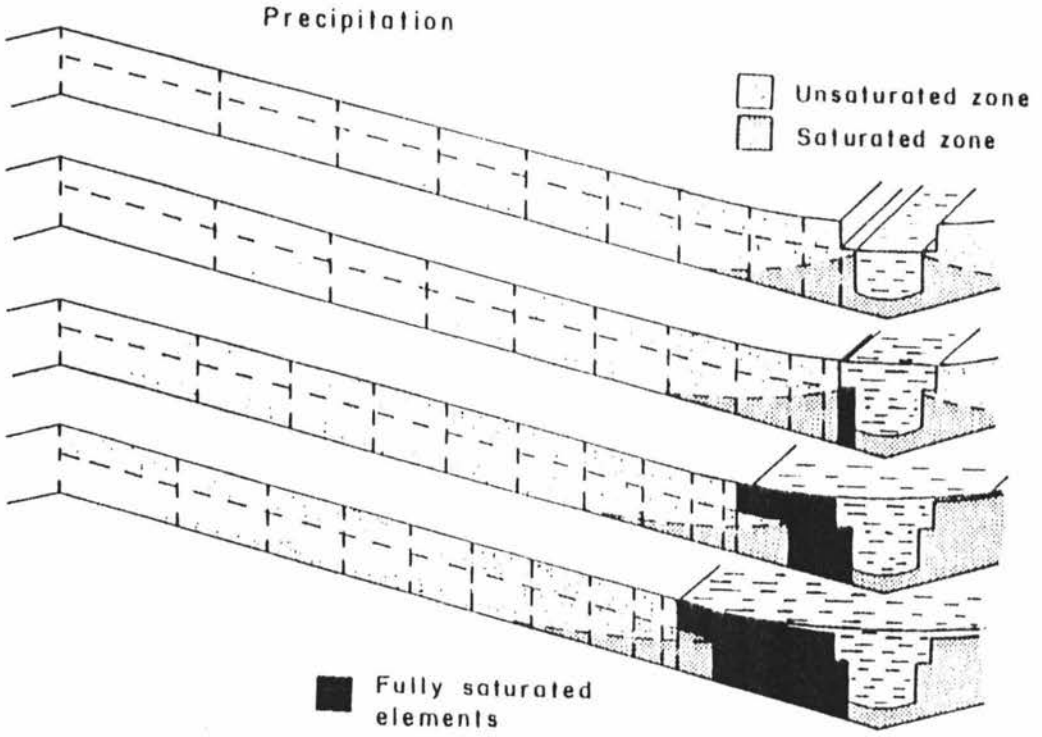

Figure 4.1 Diagram showing how the variable source area model operates under storm rainfall. As surface elements become fully saturated, storages are carried forward and the slope remaining within the zone of infiltration is redissected into 10 elements. When a surface element drains below saturation, the zone of infiltration is redissected accordingly (from Hewlett and Troendle, 1975).

equations selected from the literature (Smith, 1972; Smith and Parlange, 1978; Bear, 1972; Dunne, 1978).

The model is stochastic because the rainfall events and the hillslope parameters are defined by a set of stochastic processes (Mejia and Rodriguez-Iturbe, 1974). The need for a stochastic component arises out of the great heterogeneity that is exhibited by the soil parameters that govern the mechanisms of runoff generation on slopes. This heterogeneity, when coupled with very irregular patterns of precipitation in time and space, can create a very complex hydrologic response on a hillslope during a rainfall-runoff event.

There is now abundant field evidence to indicate that soil saturation and ponding occur on partial areas that are distributed spatially over a hillside and that the dimensions of these source areas vary through time and space within a single event and from one event to another. Freeze (1980) used a stochastic approach based on the premise that a complete deterministic description of the spatial distributions of the hillslope parameters that control source area occurrence is unattainable. He suggested that it was far more reasonable to try to assess available data in a statistical framework.

Conclusion

The discharge from a hillside or catchment is the integrated response to precipitation input. This integration extends in time and space over the area involved, and over the individual processes operating on and below the land surface. The processes include interception, ponding, evaporation, infiltration, transpiration, soil moisture storage, groundwater storage, capillary rise and the movement of water through soil.

These processes are reasonably well understood as small-scale processes taking place at, above, and under a single small area of the ground surface, and on this scale they can be expressed by mathematical equations and logical expressions. However, "for catchments of any size

and heterogeneity, the problems of sampling (including data collection and system characterization) and integration become formidable; and the beautiful economy of analytical scientific methods is soon lost in the magnitude, complexity, and imprecision of the task of synthesis" (Philip, 1975).

Scientists attempting to produce a catchment model with a physical basis are faced with a dilemma. Every basin is an exceedingly complex open system with component processes and state variables that may change rapidly over space and time. Even if the processes operating were fully understood, then an impossibly large number of parameters would be necessary to model the response of the spatially-structured system in any but the crudest manner. On the other hand, exceedingly simple models with only one or two parameters can provide a good empirical fit to the response of a particular catchment.

James (1972) has suggested that "model building combines art with science. The science comes in the theoretical derivation and empirical verification of equations describing the hydrologic processes. The art comes in reviewing the large body of available equations and supporting data and combining appropriate expressions in the manner which will give the best results".

The intention of this study was to use a physically-based model, which was not too detailed, to study the behaviour of the water table and to simulate the processes of runoff generation on sloping land. Chapter 5 describes such a simple model.

CHAPTER 5

A MODEL TO PREDICT SURFACE RUNOFF AND WATER TABLE LEVELS IN THE TOKOMARU SILT LOAM

Introduction

The model described in this chapter is based on the simple model developed by Horne (1985) for predicting water table levels in the Tokomaru silt loam. Horne used the model to predict the number of unsafe grazing days in a year on flat areas which were both undrained and pipe-mole drained. The principal modification made for this study has been the inclusion of slope as a driving force for throughflow.

A program listing and sample output are provided in Appendix B.

Physical concepts

Soil water movement occurs because of differences in the potential energy of soil water from one point to another. The hydraulic potential (ϕ) is the sum of the pressure potential (ψ) and the gravitational potential (Z). The pressure potential (ψ) is positive beneath the water table due to hydrostatic pressure, and negative above the water table due to the attractive forces between water and soil solids induced by surface tension and adsorption.

These potentials are measures of energy per unit weight of water and are usually given dimensions of length. Thus at any location, the gravitational potential (Z) can be equated with the negative value of the depth z (mm) relative to the soil surface - a suitable reference level.

Using these units we can write

$$\phi = \psi - z \qquad [11]$$

where z is the depth below the soil surface.

Horizontal water movement through a saturated isotropic soil is described by Darcy's equation which expresses the flow rate Q ($mm^3\ d^{-1}$) as a function of the saturated hydraulic conductivity of the soil K ($mm\ d^{-1}$), the hydraulic potential ϕ (mm) and the cross sectional area A (mm^2) through which flow occurs.

The equation is

$$Q = -KA\nabla\phi \qquad [12]$$

For horizontal, one dimensional flow in the x direction, this equation simplifies to

$$Q = -KA\ d\psi/dx \qquad [13]$$

The relationship between depth (z), pressure potential (ψ) and volumetric water content (θ)

To describe water movement in a soil profile, we need to know how the pressure potential (ψ) varies with depth (z), and the relationship between ψ and θ for the particular soil. For simplicity the model makes the following assumptions.

(i) Soil water above the water table is at potential equilibrium with the water table at all times.

i.e. at any location ϕ is constant with depth in the top 450 mm of the soil profile.

(ii) θ is a linear function of ψ and hysteresis is insignificant over the range of interest i.e. for $0 \geq \psi \geq -450$ mm.

(iii) There is no water movement below 450 mm once the profile has rewet in late autumn.

Using the published soil water retentivity data of Scotter *et al.*, (1979), along with assumption (ii) an expression for θ as a function of ψ was derived. Above the water table

$$\theta = a_i \psi + f_i \qquad [14]$$

where a_i (mm^{-1}) and the porosity f_i are constants for soil layer i.

Below the water table

$$\theta = f_i \qquad [15]$$

Assumption (i) leads to the following expression relating Ψ and z

$$\psi = z - T \qquad [16]$$

where T equals the depth from the soil surface to the water table in mm.

T can now be expressed as a function of W (mm), the equivalent depth of water in the soil profile.

Combining equations [14] and [16], we find θ at depth z is given by

$$\theta = a_i (z - T) + f_i \quad \text{for } z < T$$
$$\theta = f_i \quad \text{for } z \geq T \qquad [17]$$

W in the top 450 mm of soil is given by

$$W = \int_0^{450} \theta \, dz = \int_0^{T} \theta \, dz + \int_T^{450} \theta \, dz \qquad [18]$$

where $0 \leq T \leq 450$ mm. Thus

$$W = \int_0^{T} [a_i \, (z-t) + f_i] \, dz + \int_T^{450} f_i \, dz \qquad [19]$$

Integration yields a series of quadratic equations relating W and T, of the form.

$$\alpha_i \, T^2 + \beta_i \, T + (\delta_i - W) = 0 \qquad [20]$$

where α_i (mm^{-1}), β_i (dimensionless) and δ_i (mm) are the constants applicable when T is in the layer i.

Thus, given W, T may be found using

$$T = -\beta_i - [\beta_i^2 - 4\alpha_i(\delta_i - W)]^{1/2} \, / \, 2\alpha_i \qquad [21]$$

Using published soil water data for the Tokomaru silt loam (Scotter, *et al.*, 1979) the top 450 mm of the soil profile was treated as four layers with the properties given in Table 5.1.

TABLE 5.1 Soil water data for the four layers of Tokomaru silt loam under consideration, along with the value of the coefficient a_i defined by equation [14] for each layer. (After Horne, 1985)

Depth interval (mm)	i	θ at P = -500 mm	f_i	a_i (mm^{-1})
0-150	1	0.445	0.566	0.00024
150-250	2	0.390	0.486	0.00019
250-350	3	0.367	0.447	0.00016
350-450	4	0.392	0.419	0.00005

By way of example, the values of the coefficients α_1, β_1, and δ_1, are determined below for when the water table is in the first or top layer of the soil profile. Equation [19] becomes

$$W = \int_{350}^{450} (0.419)\, dz + \int_{250}^{350} (0.447)\, dz + \int_{150}^{250} (0.486)\, dz + \int_{o}^{T} [0.00024(z - T) + 0.566]\, dz \qquad [22]$$

Integration and rearrangement gives

$$0 = -0.00012T^2 + (220.1 - W) \qquad [23]$$

and so values of $-0.00012\ mm^{-1}$, 0, and 220.1 mm for α_1, β_1, and δ_1, respectively. Values for α_1, β_1, and δ_1 are shown in Table 5.2, along with the range of W for which they apply.

TABLE 5.2 **Coefficients for use in equation [21] along with range of W for which they apply. (After Horne, 1985)**

Depth interval (mm)	i	α_i (mm^{-1})	β_i	δ_i (mm)	Range of W (mm)
0-150	1	-0.00012	0	220.1	$220.1 \geq W \geq 217.4$
150-250	2	-0.000095	-0.0075	220.7	$217.4 > W \geq 212.9$
250-350	3	-0.00008	-0.015	221.6	$212.9 > W \geq 206.5$
350-450	4	-0.000025	-0.0535	222.3	$206.5 > W \geq 193.2$

A plot of equation [21] i.e. equivalent water depth in the top 450 mm of soil (W) against the depth of the water table (T) appears in Figure 5.1. Note the sensitivity of the water table height in the top 100 mm of the soil profile to any change in the water content. When the water table is at the surface a change of 1 mm in the water content due to evapotranspiration will cause the water table to drop 96 mm, whereas the next 1 mm of evapotranspiration will cause a drop of only 36 mm. Conversely for rainfall; when the water table is only 100 mm below the surface then 1 mm of rainfall will bring it to the surface.

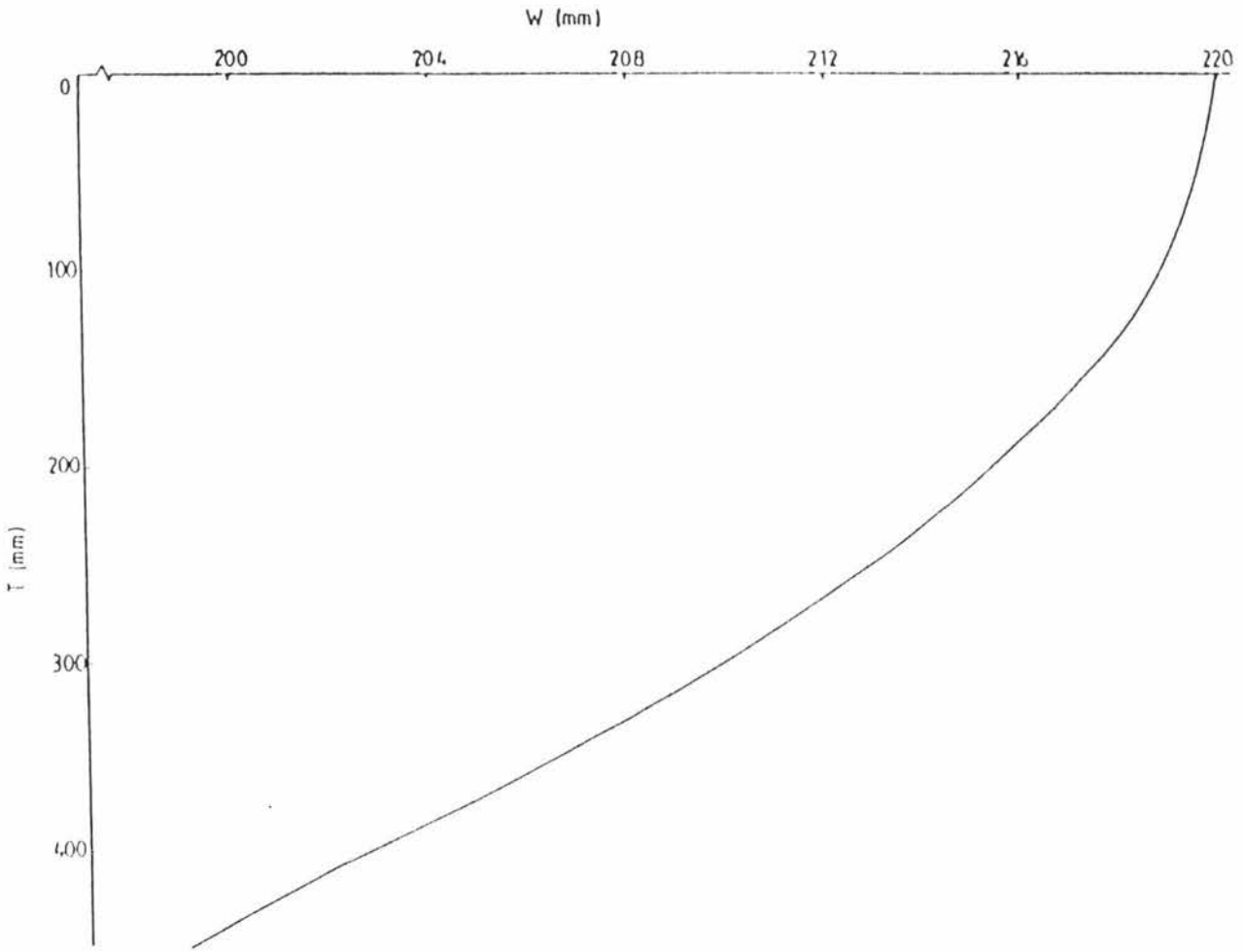

Figure 5.1 Equivalent depth of water (W) in the top 450 mm of the soil profile as a function of water table depth (T).

Evaluating the water content of the soil (W) from weather data

The change in water stored in the profile (ΔW) over any selected time interval Δt can be calculated using the following equation.

$$\Delta W = (P - E - S_r - L - U)\ \Delta t \qquad [24]$$

where
- P = rainfall (mm/day)
- E = evapotranspiration (mm/day)
- S_r = surface runoff (mm/day)
- L = lateral subsurface flow (mm/day)
- U = deep drainage (mm/day)

Rainfall and Evapotranspiration

Half-hourly, hourly or daily rainfall data are used in the model depending on whether single events or seasonal patterns are being studied. Evapotranspiration, however, is kept constant at 1 mm d^{-1} which is typical of the winter evapotranspiration rate.

Deep drainage

The Tokomaru silt loam has a very densely packed fragipan at approximately 500-700 mm depth. This impermeable subsoil restricts all or most deep drainage once the profile has wet up, so U in equation [24] can be taken as zero.

Surface Runoff

Once the soil profile is saturated, further rainfall either accumulates on the soil surface as ponded water, or becomes surface runoff (S_r). Ven Te Chow (1964) suggests that anywhere between 1 and 5 mm of water can be detained on the soil surface before runoff begins. This surface storage is attributed to unevenness in the microtopography such as hoof marks, and terracetting on sloping land.

The model assumes surface runoff will occur only when T is 1 mm above the soil surface to take surface detention into account. Following surface runoff there must be 1 mm of evapotranspiration before the water table begins to drop below the soil surface.

Thus if $W > 221.1$ then $S_r = W - 221.1$ where 221.1 mm is the sum of the equivalent depth of water in the soil profile when the water table is at the surface (220.1 mm) plus the 1 mm of water present due to surface ponding.

Lateral subsurface flow

To evaluate lateral subsurface flow it is assumed that such movement will occur only in saturated soil and that the saturated hydraulic conductivity (K) is constant with time.

For convenience the Dupuit-Forchheimer assumptions are also applied. These assumptions are that in a system of gravity flow toward a shallow sink, all the flow is parallel to the surface, and that the pressure head gradient inducing this flow is equal to the slope of the water table and so independent of the depth.

Applying the Dupuit-Forchheimer assumptions to Darcy's equation for flow parallel to a (horizontal) soil surface gives

$$Q = KA\ dT/dx \qquad [25]$$

Consider a soil segment of width w with a height h through which flow occurs. Then

$$h = z_m - T \qquad [26]$$

where z_m is the depth to the impervious layer. Substituting equation [26] into equation [25] yields the following expression for lateral subsurface flow.

$$Q = K\ w\ (z_m - T)\ dT/dx \qquad [27]$$

For water movement on sloping terrain the slope is also a driving force and equation [27] becomes

$$Q = K\ w\ (z_m - T)\ (dT/dx + \sin \sigma) \qquad [28]$$

where σ is the slope angle.

Effect of lateral subsurface flow on the water table level

To determine the volume of water flowing through the soil, the soil profile is considered as a series of segments as depicted in Figure 5.2.

The law of conservation of mass gives the following equation for the change in equivalent depth of water in segment j during time Δt,

$$\Delta W_j = \{[(Q_{j-1} - Q_j) + (R_{j-1} - R_j)] / w\Delta x + (P - E)\}\ \Delta t \qquad [29]$$

where Q_j, R_j, Q_{j-1}, R_{j-1}, P, E, w and Δx are as illustrated and defined in Figure 5.2. In the limit, as the values of W_j, Δt and Δx become very small equation [29] reduces to

$$\partial W_j/\partial t = (\partial Q_j/\partial x + \partial R_j/\partial x)/w + (P-E) \qquad [30]$$

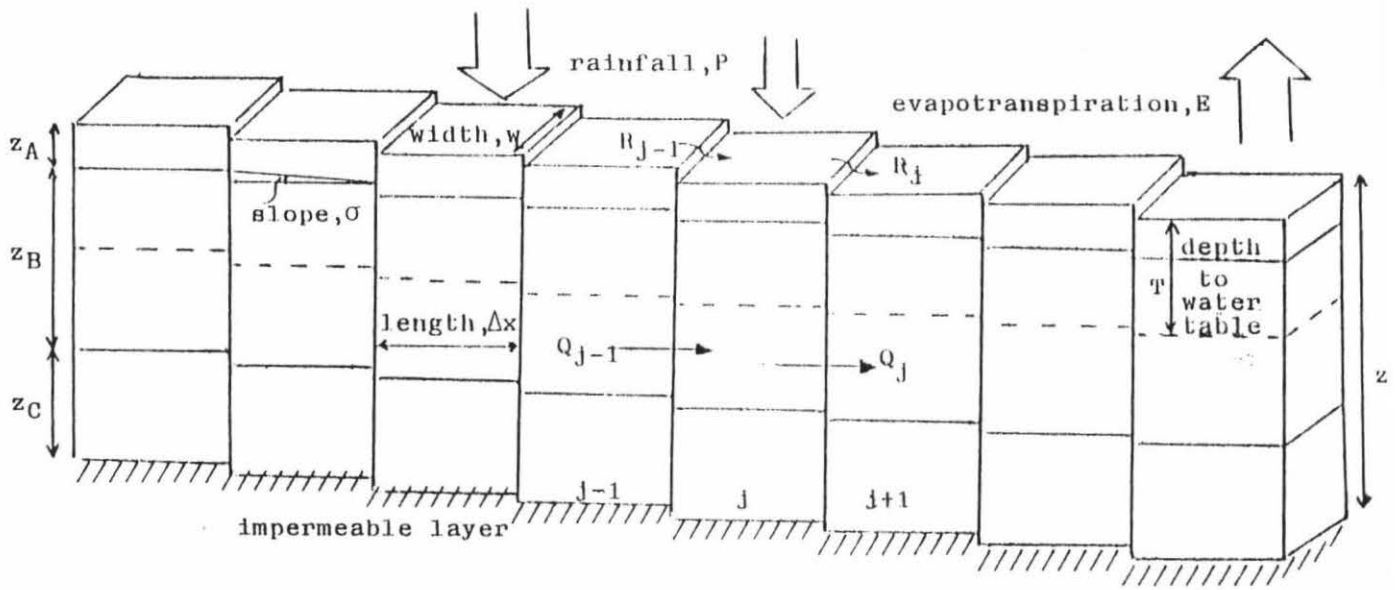

Figure 5.2 Model representation of a runoff plot. The soil was sectioned into a number of segments including j-1, j and j+1. Q_j is the rate at which water flows out of segment j, and Q_{j-1} is the rate at which water flows into segment j. R_{j-1} is the rate of surface runoff onto segment j, and R_j is the rate of surface runoff off segment j.

R_j is taken as zero unless the water table is at a level 1.0 mm above the soil surface, in which case $\partial W_j/\partial t = 0$, and so

$$\partial R_j/\partial x = -\partial Q_j/\partial x - w(P-E) \; / \; \Delta t \qquad [31]$$

The value of Q_j is given by equation [28].

To accommodate the change in saturated hydraulic conductivity with depth the soil was conceptalised as three horizons with depths Z_A, Z_B and Z_C (m), and hydraulic conductivity (K) in the x direction for each column is given by the following equations:

$$\text{If } T \geq Z_A + Z_B \text{ then } K = K_C \qquad [32]$$

$$\text{If } Z_A + Z_B > T \geq Z_A \text{ then } K = [Z_C K_C + (Z_A + Z_B - T)K_B]/(Z_m - T) \qquad [33]$$

$$\text{If } T < Z_A \text{ then } K = [Z_C K_C + Z_B K_B + (Z_A - T)K_A]/(Z_m - T) \qquad [34]$$

If the equivalent depth of water (W) is known for each column at the beginning of a simulation, along with weather data for all subsequent time intervals, then W for each column at the end of the simulation can be calculated using the equations presented above. Computations are carried out to simulate the effect of rainfall, evapotranspiration, lateral subsurface flow and surface runoff on the water content of each soil column over a short time interval. With the water content known at the end of the time interval, the water table level is calculated using equation [21] in conjunction with Table 5.2.

During each simulation the amount of rain lost from the soil columns as lateral subsurface flow and surface runoff is also computed.

CHAPTER 6

SIMULATION OF RUNOFF EVENTS AND WATER TABLE DECLINE FOR A SLOPING TOKOMARU SILT LOAM

Parameterisation of the model

Before the model described in Chapter 5 can be used to simulate the field experiment described in Chapter 3, values for hydraulic properties of the soil have to be obtained. Based on field observation and measurements the soil profile was conceptualised as the having three layers or horizons described below. Under a good pasture cover the top 50 mm has a high organic matter content and a significant volume of macropores due to biological activity. This results in a high infiltration rate and permeability. Saturated hydraulic conductivity measurements of this layer using the core method revealed K_s values ranging from 2000 to 27000 mm/day (see Chapter 3). In the model the K_{sat} value for the top 50 mm of soil was set at 6000 mm/day.

The next 250 mm (i.e. the layer between 50 and 300 mm depth) comprised the A and AB horizons, which observations indicated were still capable of conducting substantial amounts of water. This layer was assigned a K_s value of 1200 mm/day based on the data displayed in Table 3.2. The third layer, between 300 and 450 mm, contained the clay-rich B_{tg} horizon and measurements made by Scotter ***et al.*** (1985) showed its hydraulic conductivity to be of the order of only 50-200 mm/day . A K_s value of 200 mm/day was used in the model to ensure that the process of throughflow was dominant and to reduce slightly the peak volumes of surface runoff. As noted by Horne (1985) the assumed values of the hydraulic conductivity are not as critical to the performance of the model as might be expected.

Below 450 mm the fragipan was encountered and this boundary was treated in the model as impermeable.

Apart from the evapotranspiration rate (1 mm/day), and the surface detention (1 mm), the slope of the plots was the other model parameter to be set. Three slopes were selected to give the plot surface in the model a close approximation to the actual surface of the runoff plots used in the field study. For distances from the top of the plot these slopes were as follows: 0-4 m 6%, 4-10 m 12%, and 10-16 m 18%.

The model was initialised by setting the water content (W) so that a reasonably accurate simulation of the first runoff event for the year was assured. With inputs of rainfall and outputs of evapotranspiration, surface runoff and throughflow, a budget of W was run and consequentially water table levels calculated.

Predicting Runoff Events

Hourly rainfall data for the Winter/Spring periods of each year were used as inputs for the model and the occurrence and magnitude of surface runoff was calculated. Figures 6.1-6.3 show the results of these simulations in graphical form. Histograms represent the daily rainfall and runoff which was recorded, as well as the runoff predicted by the model.

In 1983, surface runoff was recorded on sixteen days between June 19 and October 7 (Julian days 170-280). Of these only four runoff events could be termed significant, that is with the volume of runoff exceeding 2 mm (200 litres/plot). The model was able to predict the occurrence of runoff on twelve of the sixteen days. The four days on which the model failed to predict any runoff included three very minor events (0.07 mm, 0.08 mm and 0.21 mm), and the last runoff event of the year (0.67 mm), where the effect of the pugging treatment (see page ...) had not been incorporated into the simulation. However, the model did predict that the water table had risen to the surface on this occasion.

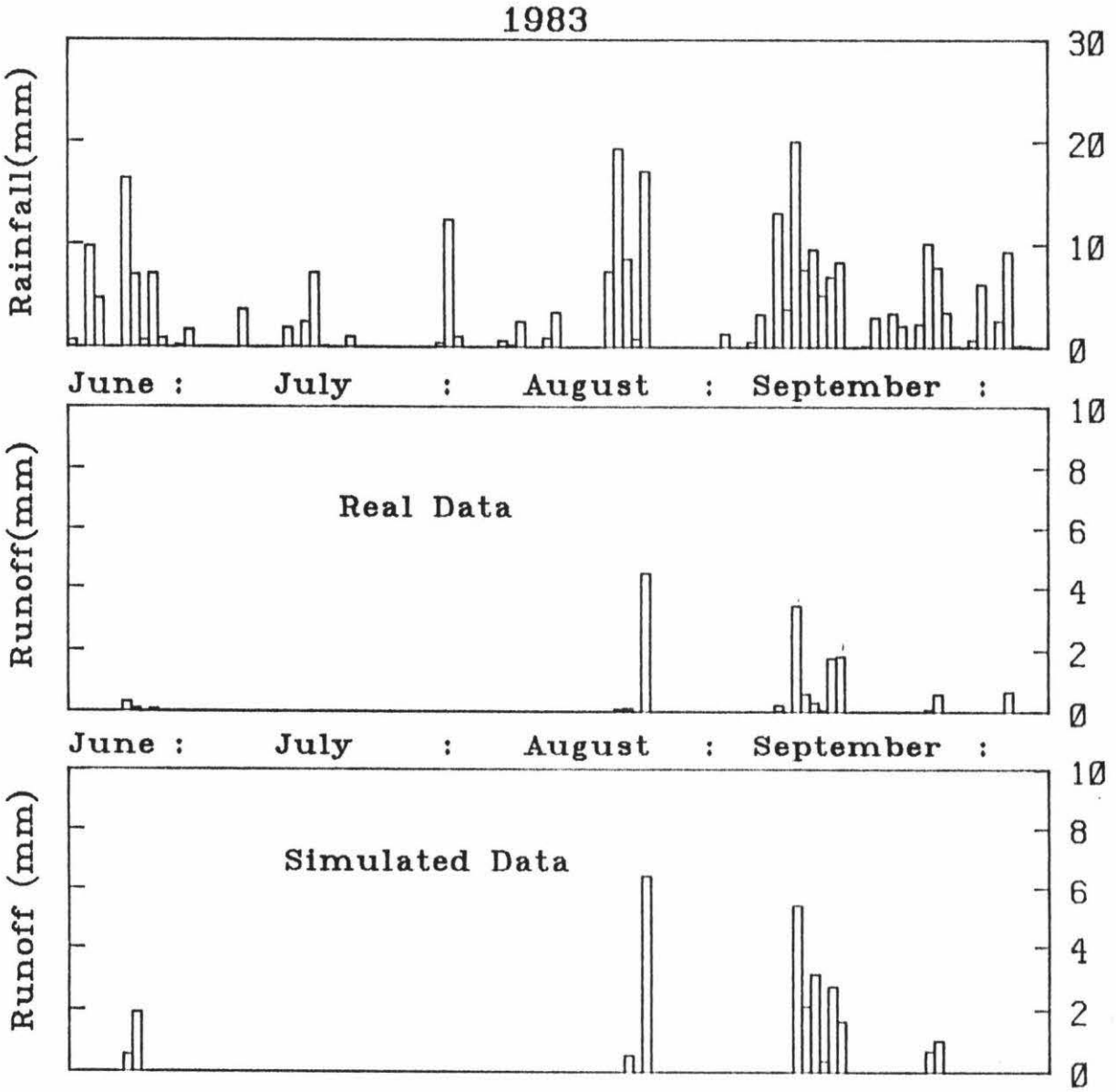

Figure 6.1 Rainfall and runoff events for Plot 1, real and simulated, during the winter/spring period of 1983.

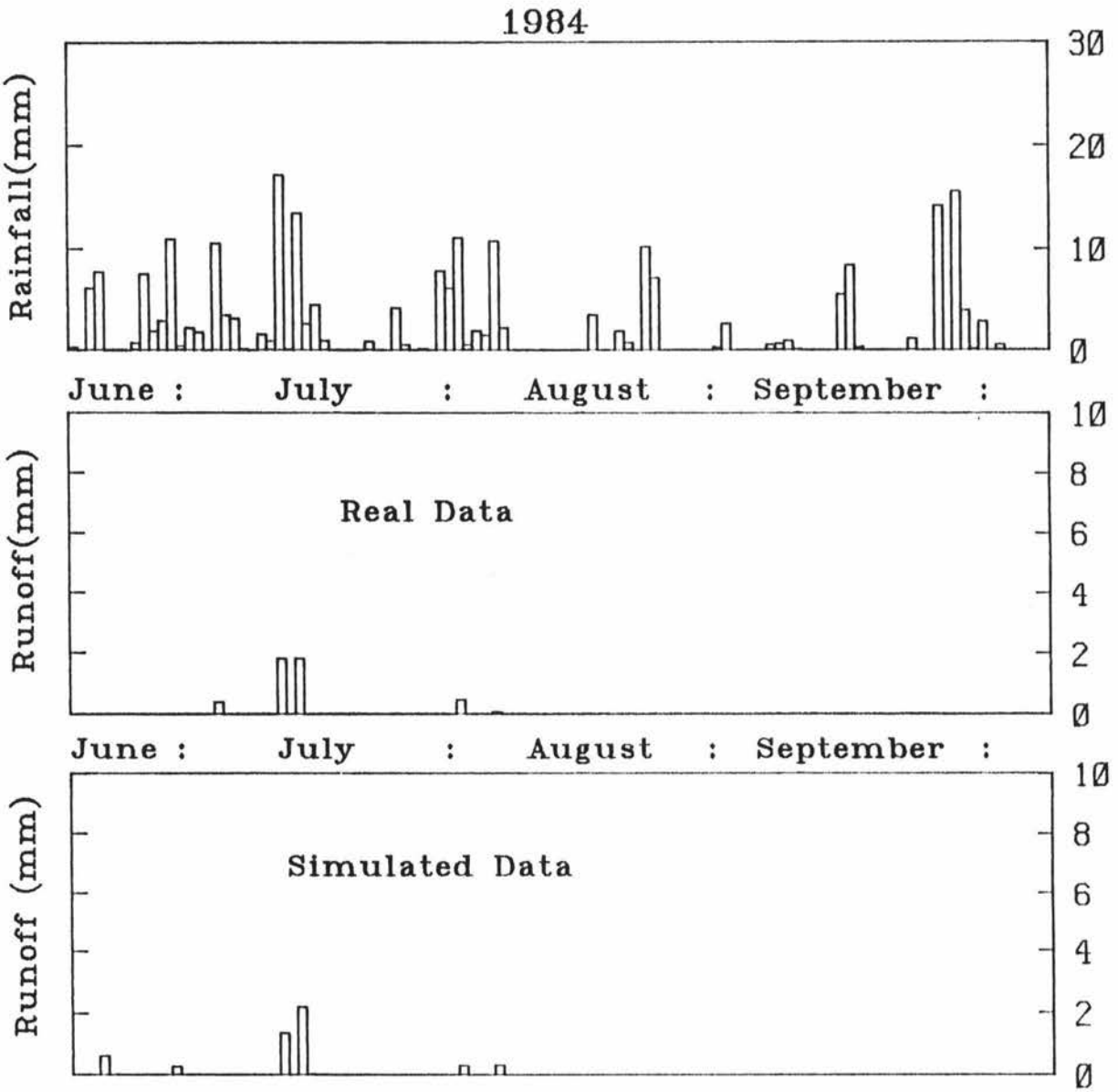

Figure 6.2 Rainfall and runoff events for Plot 1, real and simulated, during the winter/spring period of 1984.

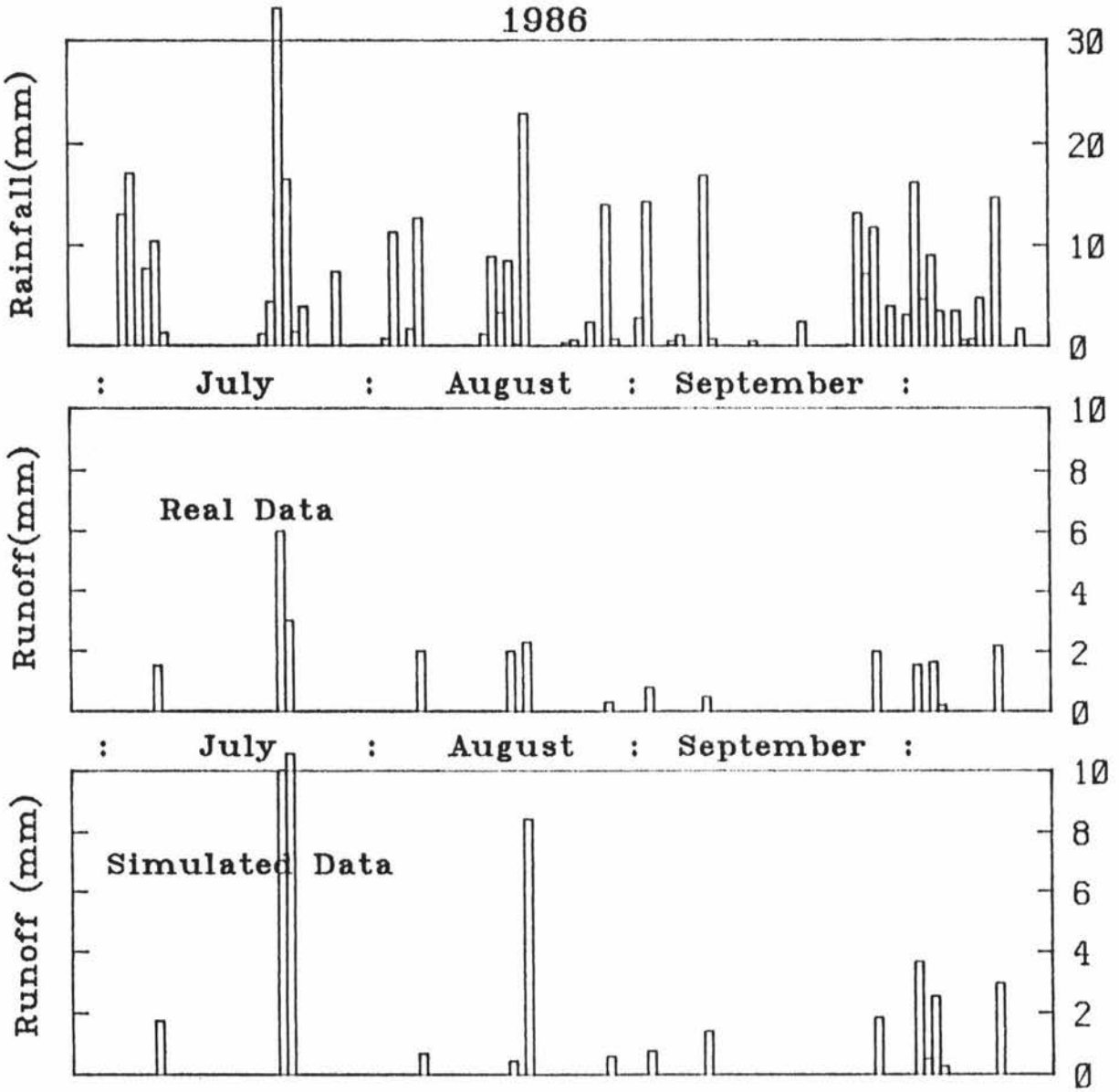

Figure 6.3 Rainfall and runoff events for Plot 1, real and simulated, during the winter/spring period of 1986.

While the timing of runoff events is predicted fairly accurately by the model, the magnitude of each event is invariably over-estimated. For example, the four major runoff events in 1983 occurred on August 23, and September 9, 13, and 14. The volumes of runoff predicted by the model on these days, with the recorded values in parentheses, were 6.4 (4.5) mm, 5.4 (3.4) mm, 2.7 (1.7) mm and 1.8 (1.6) mm. The smaller runoff events were even more at variance with the measured values than the larger ones. Such discrepancies suggest perhaps that the topsoil, especially, may be a great deal more permeable than the experimental work suggested.

Other reasons for this over-estimation could include inaccurate assessments of the surface detention, evapotranspiration, throughflow or hydraulic conductivities. All these parameters are likely to vary both temporally and spatially; and if higher values had been used for any of them in the model a reduced amount of surface runoff would have been predicted. Another factor contributing to the higher than recorded runoff could be the limitation placed on the model by the profile depth of 450 mm. In reality the depth to the restricting layer may be up to 700 mm from the surface. The restricted profile depth assumed could in turn be limiting the amount of subsurface throughflow, and therefore causing over-estimation of surface runoff.

The Winter/Spring data for 1984 are shown in Figure 6.2. While this was not a particularly wet year, the runoff events which did occur were predicted fairly accurately by the model. Data for 1985 are not shown as they are similar to 1984 with only one major storm and associated runoff.

The wet season of 1986 (Figure 6.3) was much more conducive to hydrological research, with ten significant runoff events recorded, along with four minor events. The model was able to predict the occurrence of each of the fourteen events. With regard to the amount of runoff, the simulated data were not as accurate as they might have been, again with most events being over-estimated.

The very large events on July 25/26 and August 24 seem to be most at variance with the recorded data, but the quality of the runoff data collected during these more extreme storms was not good, because of

problems associated with the overflow into the cream vats. They are shown only to complete the record.

Simulation of individual runoff events

The three storm events discussed in detail in Chapter 2 were simulated using 10 minute-interval rainfall data as input. Figures 6.4-6.6 show the hourly rainfall histogram, together with the real and simulated hydrographs from both runoff plots for the three events.

The runoff event of August 23 (Figure 6.4) resulted from saturation overland flow as explained in Chapter 2. The model simulates this process, as evidenced by the simulated hydrographs which show that peak runoff does not coincide with peak rainfall; it occurs some two hours after the highest intensity rainfall.

The shapes of the simulated hydrographs are somewhat different to the shapes of the recorded hydrographs as a consequence of the relative simplicity of the model compared to the real situation. More accurate assessment of the hydraulic conductivities, evapotranspiration rate and depths of each of the soil layers probably would have resulted in a better fitting hydrograph, but the aim of producing a simple model using easily measured parameters would not have been met.

The consistently higher runoff from Plot 2 prior to pugging was simulated in the model by adding a further four segments to the uphill end. This effectively ensured that more throughflow was generated and added to the saturated wedge at the lower end, which then resulted in more runoff.

Expressed in terms of the percentage of rainfall for each event, the amount of runoff predicted by the model was quite accurate for Plot 2 (16% for both real and simulated data), but runoff for Plot 1 was overestimated (7% for real data; 12% for simulated data). Once again, fine tuning may have improved the predictions but it was considered counter-productive.

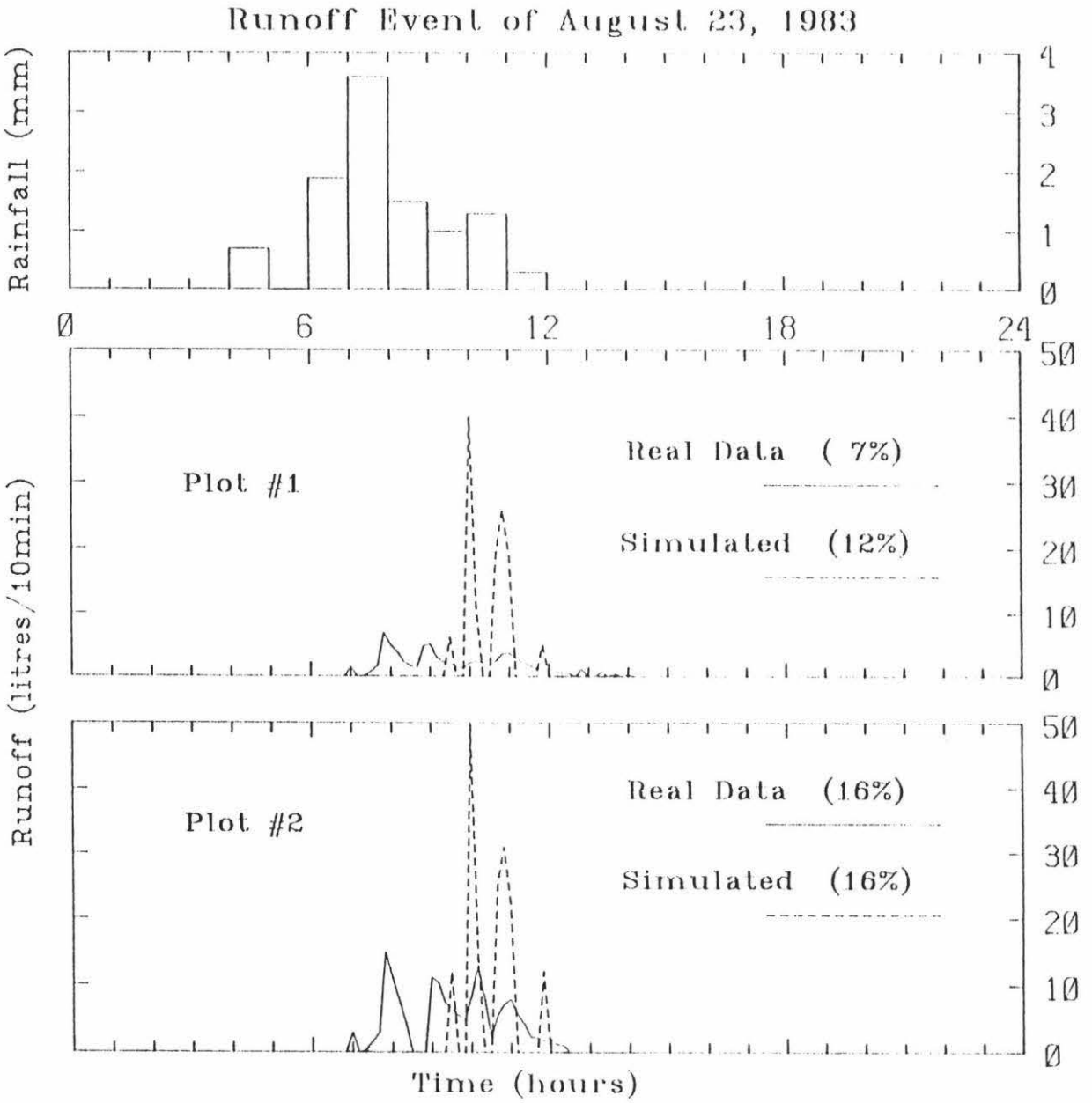

Figure 6.4 Rainfall histogram, real and simulated runoff hydrographs from Plots 1 and 2, for storm of August 23, 1983.

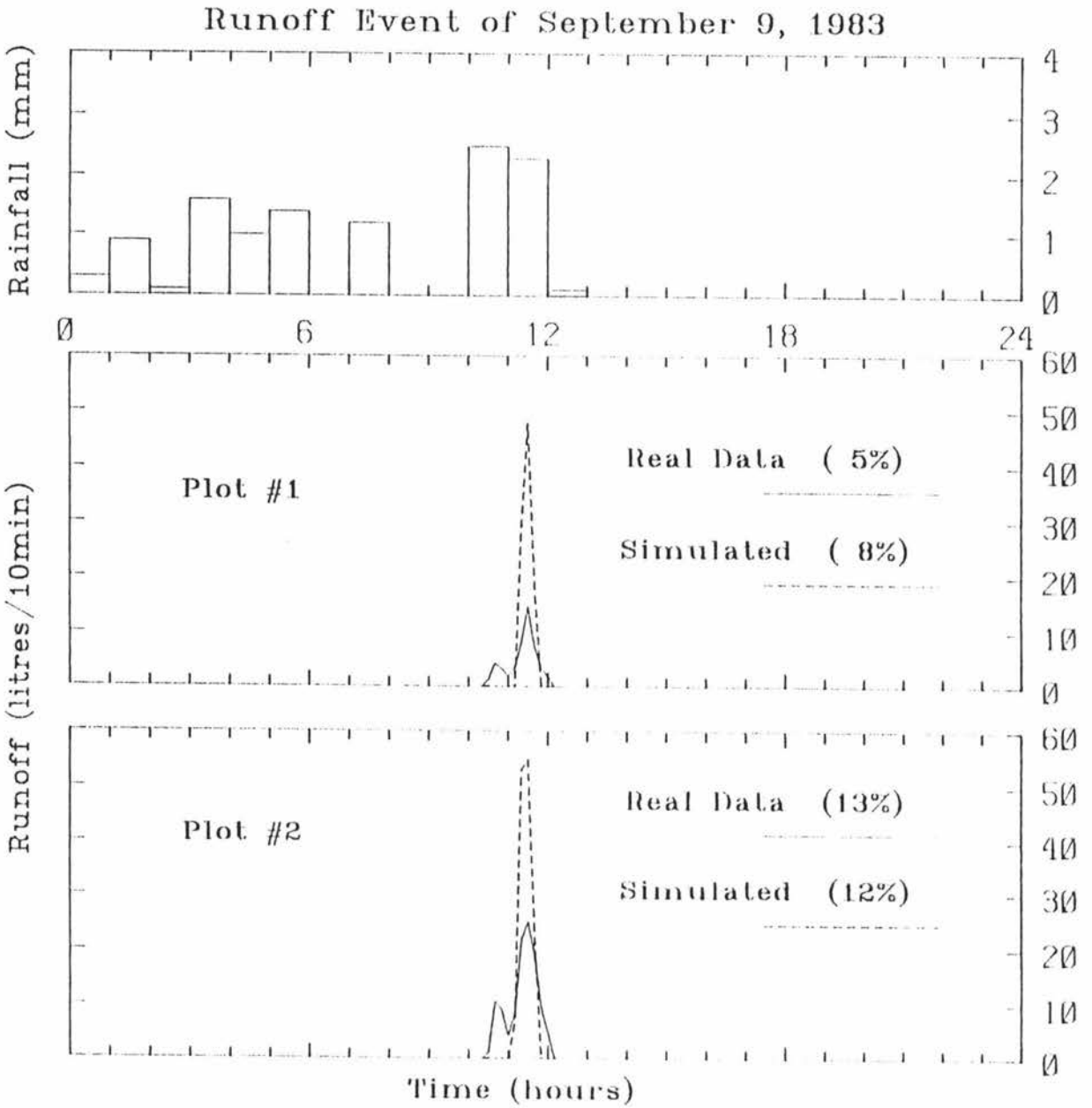

Figure 6.5 Rainfall histogram, real and simulated runoff hydrographs from Plots 1 and 2, for storm of September 9, 1983.

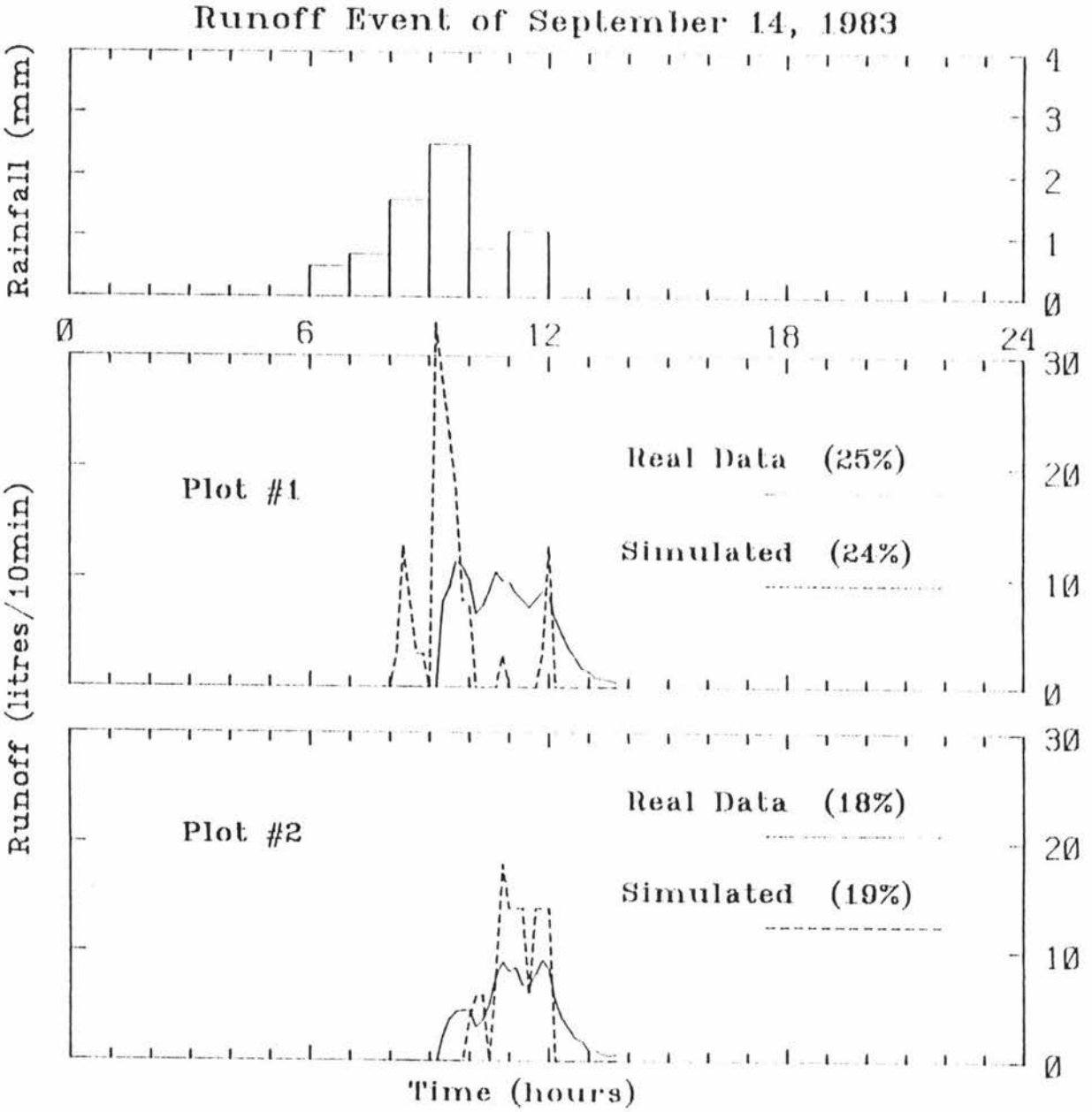

Figure 6.6 Rainfall histogram, real and simulated runoff hydrographs from Plots 1 and 2, for storm of September 14, 1983.

Figure 6.5 compares the recorded and simulated hydrographs for the runoff event of September 9. Once again the process of saturation overland flow is well illustrated with the runoff occurring only in the final stages of the storm.

The effect of pugging on infiltration and runoff

The drastic reduction in infiltration capacity caused by pugging damage, and the subsequent increase in runoff by the Hortonian process where rainfall rate exceeds infiltration rate, was easily simulated. For the storm of September 14, the K_s value of the top layer of soil in Plot 1 was set to 30 mm/day (1.2 mm/hour), and any rain falling at a greater rate than this immediately became either surface detention or runoff. In contrast, K_s for Plot 2 was left at 6000 mm/day (240 mm/hour), so only saturated overland flow occurred on that plot.

Both the recorded and simulated runoff hydrographs for the September 14 storm are shown in Figure 6.6. As the parameters for the undamaged Plot 2 were exactly the same as used previously, a typical saturation overland flow runoff hydrograph was produced. Allowing for the crude approximations used in the model the similarity between the simulated and recorded hydrographs is reasonable.

With the conductivity of the top layer of Plot 1 much reduced, the runoff hydrographs now reflect more closely the changes in rainfall intensity. The effect is particularly marked in the simulated runoff hydrograph which shows sharp peaks in runoff whenever the rainfall rate exceeds 1.2 mm/hour. While the recorded hydrograph matches maximum runoff with maximum rainfall the effect is not as marked as in the simulation. In the real situation the runoff probably includes both Hortonian and saturation overland flow, with surface roughness perhaps slowing the runoff process. The reduced infiltration is primarily a surface sealing phenomenon which is not able to be incorporated satisfactorily into the model. While the surface may be sealed over some proportion of the plot, the sealing is probably not complete and in some areas infiltration could still be taking place at rates much higher than the rainfall intensity. Furthermore, the area above the plot was not damaged by stock treading,

and rain infiltrating in that region would probably be contributing to the saturated soil layers within the plot.

Despite these limiting factors, the model was able to produce satisfactory estimates of the amounts of runoff generated from each of the plots. Runoff from the damaged Plot was recorded as being 25% of the rainfall during this storm, and the simulated runoff amounted to 24% of rainfall. Plot 2 yielded runoff amounting to 18% of rainfall and the simulated estimate was 19%.

Simulation of water table behaviour

One of the variables calculated in the model is the average depth to the water table in each soil segment. This enabled a comparison between the data collected following the runoff events of mid-July 1984 (described in Chapter 2), and the simulated data. Knowing that the water table behaved differently at transect A-B when compared with transect C-D, a reasonably accurate simulation would not only enhance the validity of the model, but would also help us to understand the processes involved in each case.

The results of the simulation, together with the measured positions of the water table, are shown in Figures 6.7 and 6.8. Along transect A-B the real water table declined at a more or less uniform rate along the transect, with the only deviation being at the lower end where a more rapid decline was probably due to a local increase in the permeability of the subsoil. This uniform rate of decline is not what one would expect if it was assumed that once rain ceased there would be no further inputs of lateral subsurface flow from above the plot. However, the wet area in the vicinity of point A at the top of the transect probably continued to have an influence on the water table for several hours after the rain stopped. This would result in the water table remaining near the surface along the greater part of the transect during the first five hours of drainage.

As was done previously, the simple way to include this behaviour in the model involved adding four extra segments of soil to the upslope section

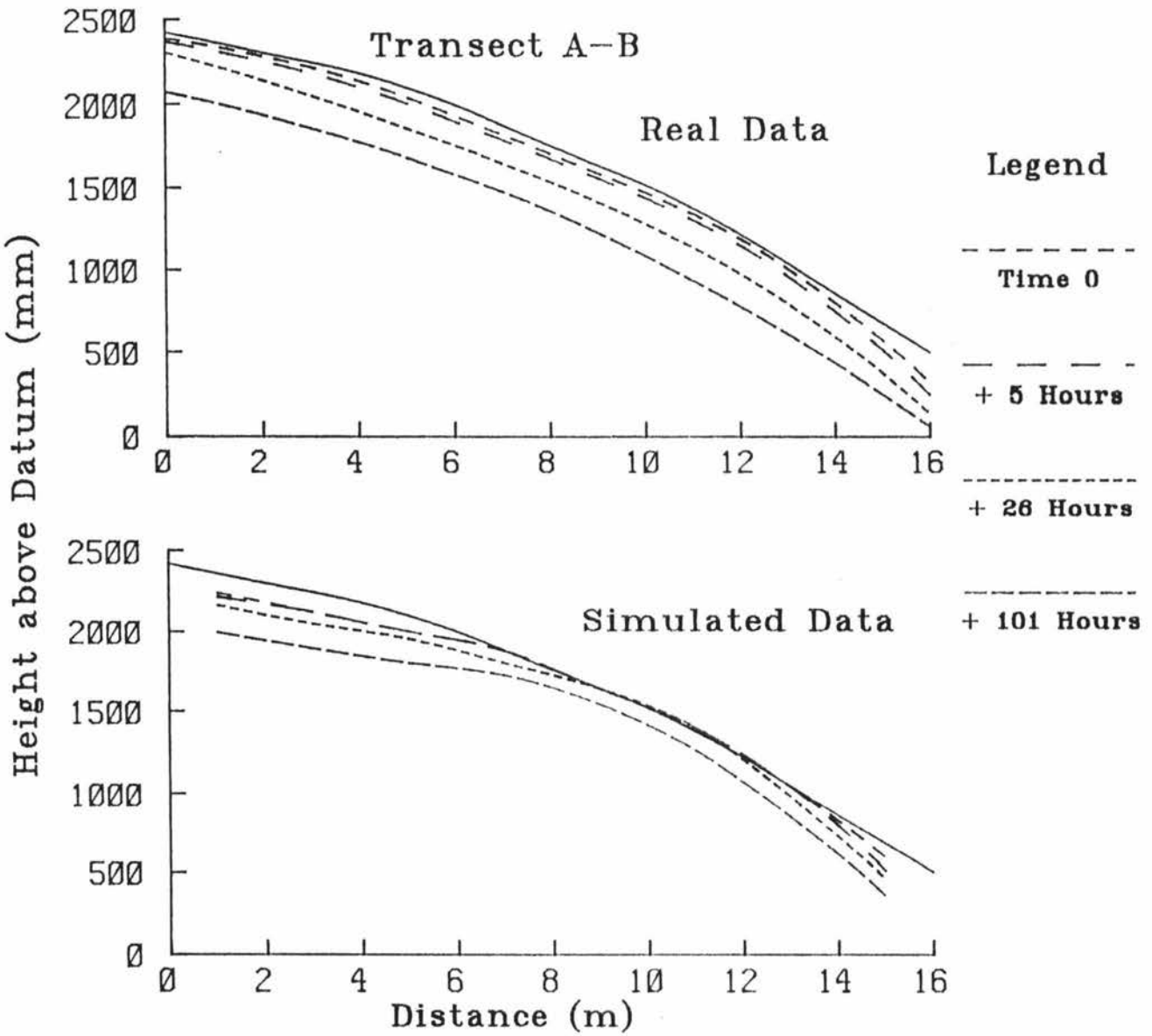

Figure 6.7 Water table decline as measured and simulated for Transect A-B, along the "uphill" side of Plot 2, following the storm events of July 12-16, 1984.

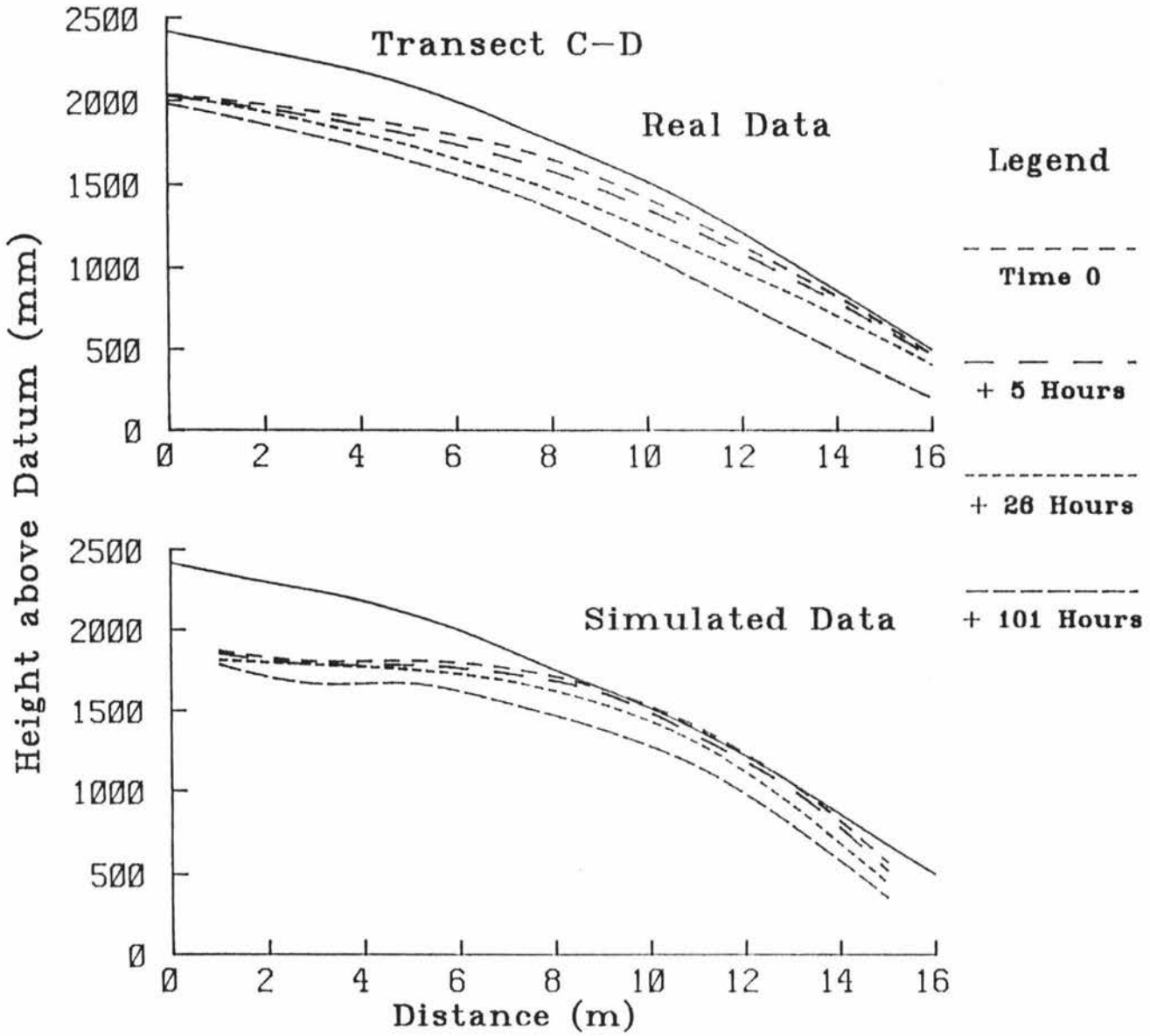

Figure 6.8 Water table decline as measured and simulated for Transect C-D, running down between Plots 1 and 2, following the storm events of July 12-16, 1984.

of the model. The simulated water table was not quite able to reproduce the steady decline along the length of the transect, but it did show two important characteristics. Firstly, the water table did remain relatively high at the top end for longer than it would have had the extra segments not been included. Secondly, the more rapid decline at the bottom end of the transect was well reproduced, indicating that the change in slope may have a greater effect than any local variation in hydraulic conductivity. The bottom two soil segments had 18% slopes compared to the 12% slopes of the preceding two segments and 6% slopes of the remaining segments.

The behaviour of the water table along transect C-D was much more as expected (Figure 6.8). Soil water drained from the top end and via lateral subsurface flow kept the water table at the lower end near to the surface for nearly a day after rain stopped. The model was able to simulate this pattern of water table decline without any modifications, suggesting that the processes involved were those already described.

For both transects the simulated data showed the water table came to the surface in the third and fourth segment from the lower end. This is perhaps an indication that the values used for K_s in the upper horizons may have been a bit lower than was actually the case. A higher evapotranspiration rate than the 1 mm/day used throughout the simulations would have also increased the rate of water table decline.

The model as an aid to understanding processes

Apart from drainage and evapotranspiration the principal driving force for saturated subsurface flow is gravity, as represented by the slope of the land. In New Zealand much of our pastoral land is located on steep slopes. Given a reasonable K_s, during the majority of storms these areas are unlikely to generate any surface runoff. The model can be used to illustrate the importance of slope angle in subsurface flow and runoff generation.

Figure 6.9 shows the recorded rainfall and simulated runoff events for the Winter/Spring period of 1983. It also shows a lateral subsurface flow hydrograph and the water table behaviour. For this simulation the slope was set at 10%. Surface runoff was predicted to have occurred on nine days, with events producing more than 5 mm of runoff occurring only twice. While the majority of subsurface flow amounted to less than 10 mm/day from the 100 m^2 plot, there were some periods when this rate was exceeded, sometimes running at 30-50 mm/day for several days.

Compare Figure 6.9 with Figure 6.10. For the latter simulation the slope has now been set at 2%. Immediately, it can be seen that there was much less subsurface flow. At no time did the rate of lateral subsurface flow exceed 10 mm/day. With less water flowing through the soil, the consequence was an increase in surface runoff. Figure 6.10 shows that this simulation resulted in 19 days with runoff, 12 of which had events producing more than 5 mm of overland flow.

Thus the model has been used to demonstrate quantitatively how steeper slopes tend to produce less surface runoff than more gentle slopes, given similar soil depth and permeability.

The importance of gravity in driving lateral subsurface flow is well illustrated.

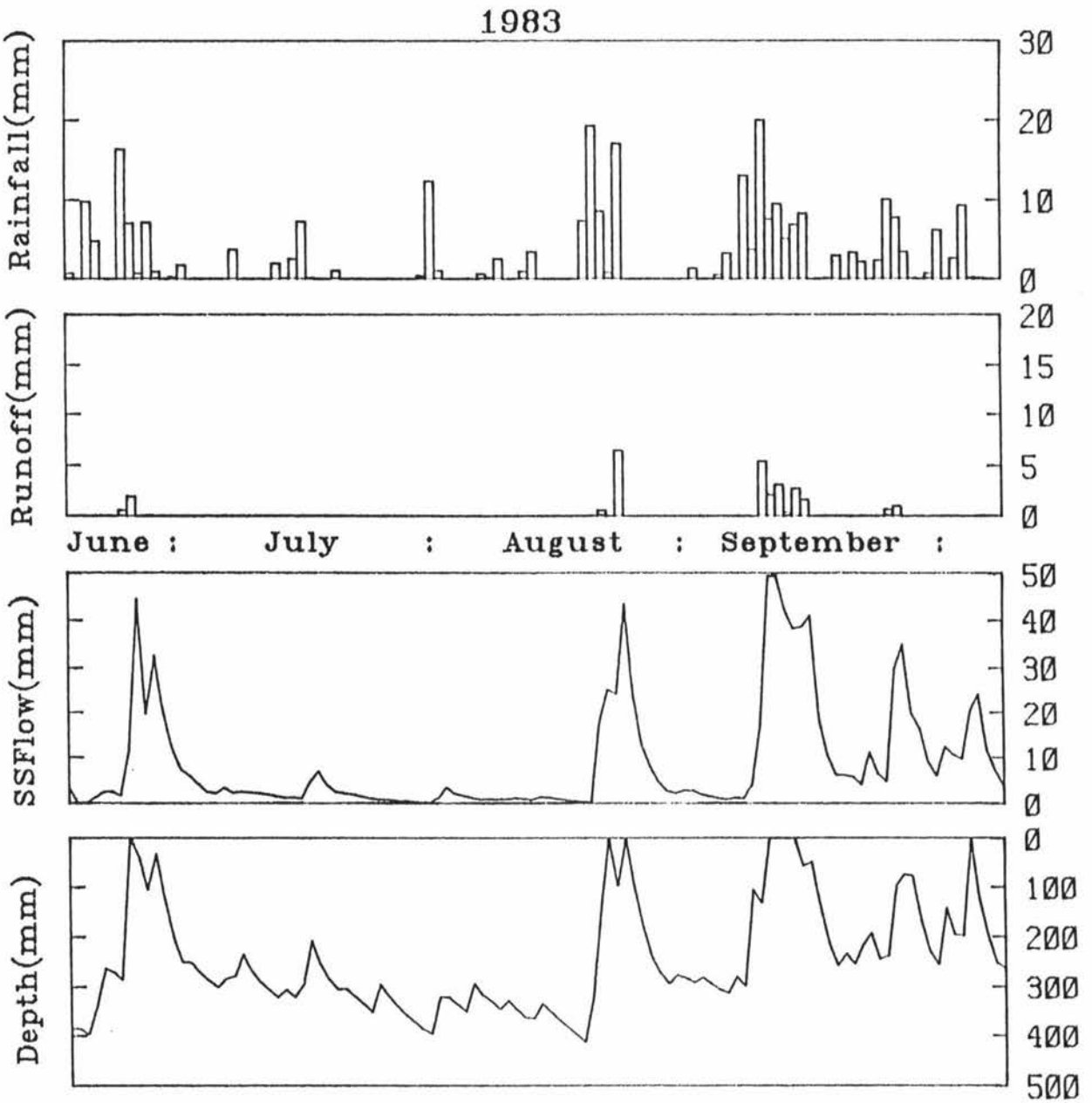

Figure 6.9 Rainfall data and simulated runoff, subsurface flow and depth to the water table (10 m downhill from the top edge of the plot) for Plot 1 over the winter/spring period of 1983.

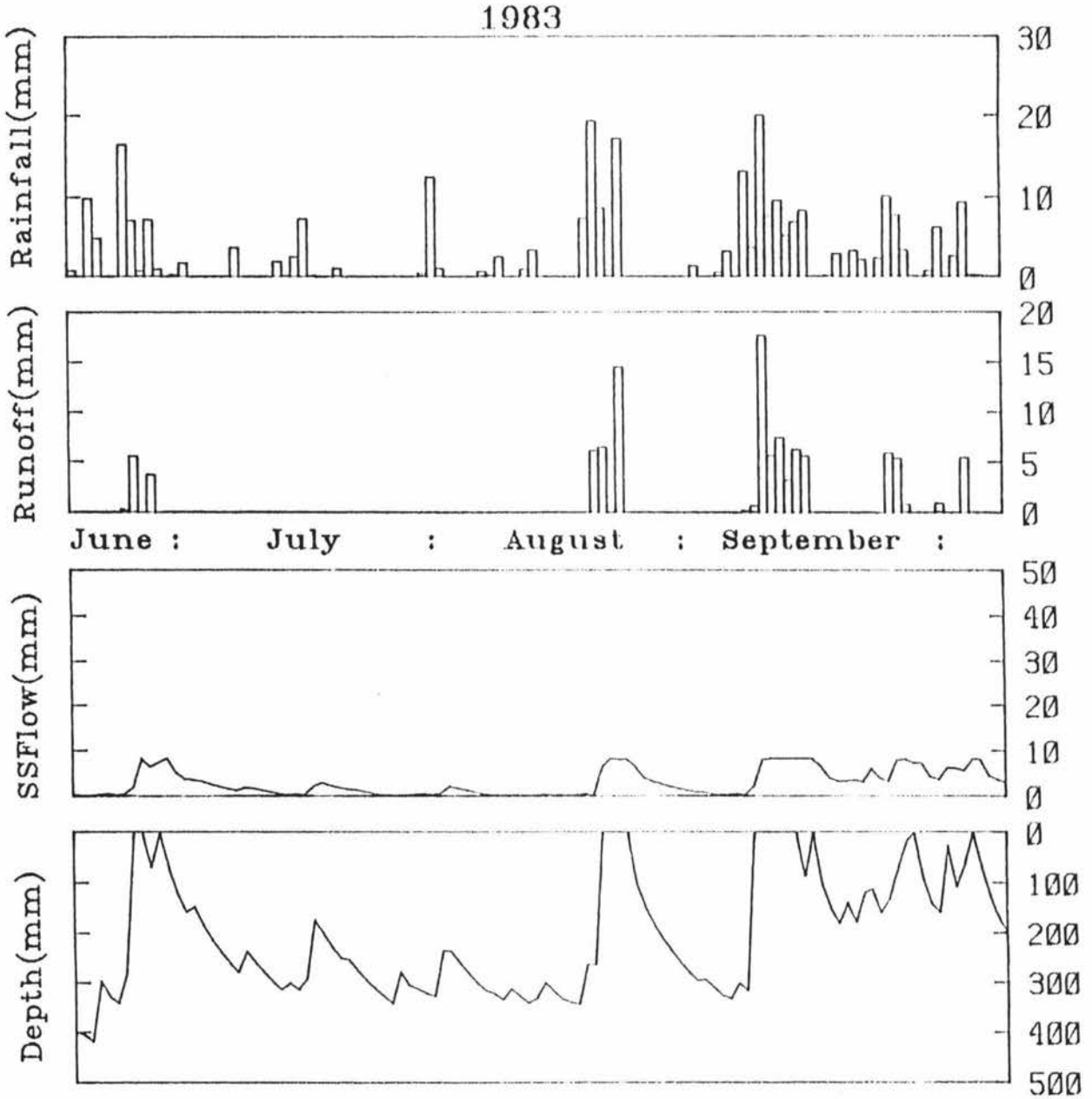

Figure 6.10 Rainfall data and simulated runoff, subsurface flow and depth to the water table (10 m downhill from the top edge of the plot) for a hypothetical plot with a 2% slope over the winter/spring period of 1983.

CHAPTER 7

CONCLUSION

To the extent that the site chosen was typical, the study supports the observation that the majority of winter rain falling on New Zealand's hillsides travels downslope via subsurface flow. Throughout the four years of monitoring storm events, surface runoff was recorded on only forty occasions, and the majority of these events were relatively minor with less than 1 mm of surface runoff being generated.

On most of those occasions when surface runoff did occur, it was as a result of the soil reaching saturation. Thus the process of saturation overland flow, rather than Hortonian flow, was primarily responsible for runoff generation.

Under conditions normally found at the study site, i.e. a good pasture sward and normal (low) intensity rainfall, the infiltration rate of the soil was not exceeded by the rainfall rate. However, when heavy stocking resulted in pugging damage and a consequent reduction in infiltration capacity, the process of Hortonian runoff became significant.

An interesting aspect of the pugging experiment was the rapid recovery of both pasture growth and the infiltration capacity of the soil. Within a month the surface crusting effect had gone, and by the following winter the infiltration rate was once again as high as it had been prior to the pugging damage being inflicted.

The behaviour of the water table on the hillslope confirmed the dominance of the process of subsurface flow in transporting water downslope. The most common sequence of events was for the water table to rise during a rainstorm, but only to within 50 - 100 mm of the surface. The hydraulic

conductivity in this layer was high enough to enable the downslope drainage of excess water. After the rain had stopped the water table would decline, over a period of three to four days, to its pre-storm depth of 400 - 600 mm; the position it maintained throughout most of the winter/spring period.

A simple, physically-based, mathematical model was developed to simulate both the behaviour of the water table, and the processes of runoff generation on sloping land. The model was able to predict quite accurately the water table behaviour during and following a rainstorm. Using hourly rainfall data, the occurrence and magnitude of runoff events over a winter/spring period were also successfully simulated.

For individual storm events, ten-minute interval rainfall data were used, and although the amount of runoff was predicted reasonably well, the shapes of the hydrographs were not always similar to the recorded data. The model was, however, able to simulate very easily the effect of markedly decreasing the infiltration capacity of the surface soil. The resulting change in the hydrograph shape showed clearly that the Hortonian process of runoff generation was operating.

Finally, the model was useful in gaining a better understanding of hillslope hydrological processes. The phenomenon whereby steeper slopes tend to produce less surface runoff than more gentle slopes, given similar soil depth, permeability and slope length, was well illustrated.

APPENDIX A

LIST OF SYMBOLS

A	cross-sectional area	$[L^2]$
D	soil water diffusivity	$[L^2T^{-1}]$
E	evapotranspiration rate	$[LT^{-1}]$
K_s	saturated hydraulic conductivity	$[LT^{-1}]$
L	lateral subsurface runoff rate	$[LT^{-1}]$
P	rainfall rate	$[LT^{-1}]$
Q	flow rate	$[L^3T^{-1}]$
R	surface runoff rate	$[LT^{-1}]$
S	sorptivity	$[LT^{-\frac{1}{2}}]$
S_a	available water storage	[L]
S_r	surface runoff rate averaged over area of interest	$[L^3T^{-1}]$
S_w	relative saturation	
T	depth to water table	[L]
U	deep drainage rate	$[LT^{-1}]$
W	equivalent depth of water in the soil profile	[L]
Z	gravitational potential	[L]
a,b	fitted parameters for various infiltration equations cited in Chapter 4	
a_i	constant relating θ and ψ for soil layer i	$[L^{-1}]$
f	porosity	
h	height of soil segment through which water flows	[L]
i	infiltration rate	$[LT^{-1}]$
k	hydraulic conductivity	$[LT^{-1}]$
n	number of measurements	
q	flux density of water	$[LT^{-1}]$
r	radius of infiltration ring	[L]
s	standard deviation	
t	time	[T]

t_p	time to ponding	[T]
w	width of soil segment	[L]
x	distance	[L]
z	depth	[L]
z_m	depth to impervious layer	[L]
α, β, δ	constants relating W and T	
ψ	pressure potential	[L]
ϕ	hydraulic potential	[L]
σ	slope	
θ	volumetric water content	

APPENDIX B -

PROGRAMME LISTING

```
      program wtable

      external openfile, stop, title

      intrinsic float, sqrt

      integer interval, delta, no_cols, no_days, no_ints, count,
     *        i, j, k, m, n, q

      real  width, length, s1, s2, s3, s4, rain, drunoff, start

      parameter ( width = 6000, length = 2000)

      integer    time(  3000)

      real     runoff(  3000),
     *      interflow(  3000),
     *       rainfall(  3000),
     *   net_rainfall(  3000),
     *          depth(    50),
     *           flow(    50),
     *           cond(    50),
     *       overflow(    50),
     *           surf(    50),
     *            dad(    50),
     *             wt(    50),
     *         water(0:3000,0:50),
     *     condA, condB, condC, A, B, C, KA, KB, KC

      common //time,runoff,interflow,rainfall,net_rainfall,water

      call title ('SIMULATION OF HILLSLOPE HYDROLOGY')

      call openfile (5,' ','read')
      call openfile (6,' ','write')
      call openfile (7,' ','write')
      call openfile (8,' ','write')
      call openfile (9,' ','write')
      write (1,200)

Comment: Read no_days (duration of simulation), interval (time between
Comment: calculations) & delta (no. of intervals between outputs)_____

      read (5,100) no_days, interval, delta

Comment: Read no_cols, m, n, q, & start (initial WT depth)_____

      read (5,101) no_cols, m, n, q, start
```

```
Comment: Read slope and hydraulic conductivities ____________________________

      read (5,102) s1, s2, s3, s4, KA, KB, KC

Comment: Read rainfall data ____________________________________________________

      no_ints = no_days * delta

      do 15 i = 1, no_ints
         read (5,103) time(i), rainfall(i)
   15 continue

Comment:  Initialise hydrological conditions____________________________________

      do 5 i = 1,no_ints
             runoff(i) = 0
         interflow(i) = 0
      net_rainfall(i) = 0
    5 continue

                count = 0
              drunoff = 0

      do 10 j = 1,no_cols
              depth(j) = 0
            water(0,j) = start
            water(1,j) = start
               flow(j) = 0
           overflow(j) = 0
   10 continue

Comment: Write output headings _________________________________________________

          write (6, 206) 'Slopes:', s1, s2, s3, s4, ' Conductivities:',
     *      KA, KB, KC, ' No. Days/Hours :',  no_days, ' No. columns:',
     *               no_cols, ' m:', m,' n:', n,' q:', q
          write (6, 207) 'Water in profile at beginning of simulation :',
     *               start, ' Interval :', interval, ' Delta :', delta
          write (6, 201)
          write (6, 226) 'Time Rain    Flow'

          write (7, 206) 'Slopes:', s1, s2, s3, s4, ' Conductivities:',
     *      KA, KB, KC, ' No. Days/Hours :',  no_days, ' No. columns:',
     *               no_cols, ' m:', m, ' n:', n, ' q:', q
          write (7, 207) 'Water in profile at beginning of simulation :',
     *               start, ' Interval :', interval, ' Delta :', delta
          write (7, 201)
          write (7, 227) 'Time Rain    Height above datum'
```

```
      write (8, 206) 'Slopes:', s1, s2, s3, s4, ' Conductivities:',
     *    KA, KB, KC, ' No. Days/Hours :', no_days, ' No. columns:',
     *             no_cols, ' m:', m, ' n:', n, ' q:', q
      write (8, 207) 'Water in profile at beginning of simulation :',
     *             start, ' Interval :', interval, ' Delta :', delta
      write (8, 201)
      write (8, 228) 'Time Rain    Depth to water table'

      write (9, 206) 'Slopes:', s1, s2, s3, s4, ' Conductivities:',
     *    KA, KB, KC, ' No. Days/Hours :', no_days, ' No. columns:',
     *             no_cols, ' m:', m, ' n:', n, ' q:', q
      write (9, 207) 'Water in profile at beginning of simulation :',
     *             start, ' Interval :', interval, ' Delta :', delta
      write (9, 201)
      write (9, 229) 'Time Rain    Water                Depth
     *             Flow/1000         Interflow   Runoff'
```

Comment: Calculate net rainfall

```
      do 16 i = 1, no_ints
       net_rainfall(i) = rainfall(i)/interval - 0.0007
   16 continue
```

Comment: Calculate hydraulic conductivity

```
      condA = KA / 1440
      condB = KB / 1440
      condC = KC / 1440


      do 90 i = 1, no_ints

      do 20 j = 1,no_cols
         if (depth(j).gt.450) then
              cond(j) = 0
         elseif (depth(j).gt.300) then
              cond(j) = condC
         elseif (depth(j).gt.50) then
              cond(j) = (condC * 150 + condB *
     *             (300 - depth(j))) / (450 - depth(j))
         else
              cond(j) = (condC * 150 + condB * 250 + condA *
     *             (50 - depth(j))) / (450 - depth(j))
         endif

   20 continue
```

Comment: Calculate interflow

```
       flow(no_cols) = cond(no_cols) * s4 * width *
     *             (450 - depth(no_cols))
```

```
      do 30 j = 1, no_cols - 1

         if     (j.le.(no_cols-m)) then
              slope = s1
         elseif (j.le.(no_cols-n)) then
              slope = s2
         elseif (j.le.(no_cols-q)) then
              slope = s3
         else
              slope = s4
         endif

         flow(j) = (cond(j+1) + cond(j)) / 2 * width
     *                 * ((depth(j+1) - depth(j)) /
     *                         length + slope)
     *                 * (450 - (depth(j+1)
     *                               + depth(j)) / 2)


         if     (j.le.q) then
               slope = s4
         elseif (j.le.n) then
               slope = s3
         elseif (j.le.m) then
               slope = s2
         else
               slope = s1
         endif


         surf(no_cols) = 500
         surf(no_cols-j) = length * slope + surf(no_cols+1-j)

    30 continue

      interflow(i) =  flow(no_cols) * interval / length / width

Comment: Calculate depth to water table ____________________________________

      do 40 j = 1,no_cols

         if (j.eq.1) then
            water(i,1) = water(i-1,1) - (flow(1) / length / width)
     *         * interval + net_rainfall(i) * interval

         else
            water(i,j) = water(i-1,j) + (flow(j-1) - flow(j))
     *                   / length / width * interval
     *              + net_rainfall(i) * interval + overflow(j-1)
         endif

         overflow(j) = 0
```

```
      if  (water(i,j).gt.221.1) then
           overflow(j) = water(i,j) - 221.1
           water(i,j) = 221.1
           depth(j) = 220.1 - water(i,j)
           go to 35
      elseif ((water(i,j).le.221.1).and.(water(i,j).ge.220.1)) then
           depth(j) = 220.1 - water(i,j)
           go to 35
      elseif ((water(i,j).lt.220.1).and.(water(i,j).ge.217.4)) then
           A = -0.00012
           B = 0
           C = (220.1 - water(i,j))
      elseif ((water(i,j).lt.217.4).and.(water(i,j).ge.212.9)) then
           A = -9.5E -5
           B = -0.0075
           C = (220.7 - water(i,j))
      elseif ((water(i,j).lt.212.9).and.(water(i,j).ge.206.5)) then
           A = -8E -5
           B = -0.015
           C = (221.6 - water(i,j))
      elseif ((water(i,j).lt.206.5).and.(water(i,j).ge.193.2)) then
           A = -2.5E -5
           B = -0.0535
           C = (222.3 - water(i,j))
      else
           A = -1
           B = 450
           C = 0
      endif

      depth(j) = (-B -sqrt(B * B - 4*A*C)) / 2 / A

35    if (depth(j).lt.0.0) then
      depth(j) = 0.0
      endif

      dad(j)  = surf(j) - depth(j)
      wt(j)   = - depth(j)

40 continue

Comment: Calculate runoff _____________________________________________

     runoff(i) = overflow(no_cols)/no_cols
       drunoff = drunoff + runoff(i)
         rain  = rain + rainfall(i)
         count = count +1
     if (count.lt.delta) go to 90
```

```
Comment: Write output file ____________________________________________

         write (6, 201)
         write (6, 205) time(i), rain,
     *                  (flow(j)/1000, j = 1,no_cols)

Comment: Write second output file _____________________________________

         write (7,205) time(i), rain,
     *                  (cond(j)*1000, j=1,no_cols)

Comment: Write third output file ______________________________________

         write (8,205) time(i), rain,
     *                  (wt(j), j = 1,no_cols)

Comment: Write fourth output file _____________________________________

         write (9,210) time(i), rain,
     *           water(i,1), water(i,no_cols-4), water(i,no_cols),
     *           depth(1), depth(no_cols-4), depth(no_cols),
     *           flow(1)/1000, flow(no_cols-4)/1000, flow(no_cols)/1000,
     *                  interflow(i), drunoff

         count = 0
          rain = 0
       drunoff = 0

   90 continue

Comment: End program _________________________________________________

       call stop(0)

Comment: Format statements ___________________________________________

   100 format( 3I4 )
   101 format( 4I4,F5.1 )
   102 format( 7F7.3 )
   103 format( I4, F4.1 )

   200 format( )
   201 format( ' ' )
   202 format( A123 )
   203 format( A122 )
   204 format( I5, 15F7.1, 2F9.2 )
   205 format( I4, F5.1, 16F7.1 )
   206 format( A7, 4F5.2, A16, 3F6.1, A17, I4, A13, I3, 3(A3, I2))
   207 format( A45, F5.1, A11, I4, A8, I4 )
   210 format( I5, F6.1, 9F7.1, F12.2, F7.2 )
   226 format( A17 )
   227 format( A31 )
   228 format( A33 )
   229 format( A93 )

       end
```

SAMPLE OUTPUT

No. of Days/Hours : 144 Interval : 10 Delta : 1
No. columns : 8 m: 8 n: 4 q: 2
Slopes: 0.01 0.06 0.12 0.18
Water in profile at beginning of simulation : 213.5
Depths of soil layers (mm) : 50 300 450
Conductivities : 6000.0 1200.0 200.0
Surface detention : 1.0 mm Evapotranspiration : 1.0 mm

Time	Rain	Runoff	SSFlow	Water	Height above datum							
10		0.	56.	213.1	249.	239.	235.	239.	235.	239.	239.	246.
20	0.00	0.	12.	213.0	251.	239.	235.	239.	235.	239.	239.	247.
30	0.00	0.	12.	213.0	253.	239.	234.	239.	234.	239.	239.	249.
40	0.00	0.	12.	212.9	255.	240.	233.	239.	233.	239.	239.	250.
50	0.00	0.	12.	212.8	258.	240.	233.	239.	233.	239.	239.	251.
100	0.00	0.	12.	212.7	260.	241.	232.	239.	232.	239.	240.	253.
110	0.00	0.	12.	212.6	262.	241.	231.	239.	231.	239.	240.	254.
120	0.00	0.	11.	212.6	264.	242.	231.	239.	231.	239.	240.	255.
130	0.00	0.	11.	212.5	266.	242.	230.	239.	230.	239.	240.	257.
140	0.00	0.	11.	212.4	268.	243.	230.	239.	229.	239.	240.	258.
150	0.00	0.	11.	212.3	270.	244.	229.	239.	229.	239.	240.	259.
200	0.00	0.	11.	212.3	272.	244.	229.	239.	228.	239.	241.	260.
210	0.00	0.	11.	212.2	273.	245.	228.	239.	228.	239.	241.	261.
220	0.00	0.	10.	212.1	275.	246.	228.	239.	227.	239.	241.	263.
230	0.00	0.	10.	212.1	277.	246.	227.	239.	226.	239.	241.	264.
240	0.00	0.	10.	212.0	279.	247.	227.	239.	226.	239.	241.	265.
250	0.00	0.	10.	212.0	280.	248.	226.	239.	225.	239.	241.	266.
300	0.00	0.	10.	211.9	282.	249.	226.	239.	225.	239.	241.	267.
310	0.00	0.	10.	211.8	284.	249.	225.	239.	224.	239.	242.	268.
320	0.00	0.	10.	211.8	285.	250.	225.	239.	223.	239.	242.	269.
330	0.00	0.	10.	211.7	287.	250.	225.	239.	223.	239.	242.	270.
340	0.00	0.	9.	211.7	288.	251.	224.	239.	222.	239.	242.	271.
350	0.00	0.	9.	211.6	290.	252.	224.	239.	222.	239.	242.	272.
400	0.00	0.	9.	211.6	291.	253.	224.	238.	221.	239.	242.	273.
410	0.20	0.	9.	211.7	289.	250.	219.	235.	217.	235.	239.	270.
420	0.20	0.	9.	211.9	287.	248.	215.	231.	212.	231.	235.	268.
430	0.30	0.	10.	212.1	284.	244.	208.	225.	205.	225.	229.	263.
440	0.00	0.	10.	212.0	286.	245.	208.	224.	204.	225.	230.	264.
450	0.00	0.	10.	212.0	287.	246.	208.	224.	204.	225.	230.	265.
500	0.00	0.	10.	211.9	289.	247.	208.	224.	203.	225.	230.	266.
510	0.00	0.	10.	211.9	290.	247.	208.	224.	202.	225.	230.	267.
520	0.00	0.	10.	211.8	292.	248.	207.	224.	202.	225.	230.	268.
530	0.00	0.	10.	211.8	293.	249.	207.	224.	201.	225.	230.	269.
540	0.00	0.	10.	211.7	294.	250.	207.	223.	201.	224.	231.	270.
550	0.00	0.	9.	211.7	296.	251.	207.	223.	200.	224.	231.	271.
600	0.00	0.	9.	211.6	297.	252.	207.	223.	199.	224.	231.	272.
610	0.00	0.	9.	211.6	298.	253.	207.	223.	199.	224.	231.	272.
620	0.00	0.	9.	211.5	300.	254.	207.	223.	198.	224.	231.	273.
630	0.00	0.	9.	211.5	301.	255.	207.	223.	198.	224.	231.	274.
640	0.00	0.	9.	211.4	302.	256.	207.	222.	197.	223.	231.	275.
650	0.90	0.	9.	212.3	289.	241.	187.	203.	175.	204.	213.	260.
700	1.00	0.	11.	213.3	274.	223.	162.	180.	148.	182.	192.	243.

710	0.50	0.	13.	213.7	267.	214.	148.	168.	132.	169.	180.	235.
720	0.30	0.	14.	213.9	264.	209.	139.	159.	121.	161.	173.	230.
730	1.00	0.	14.	214.9	249.	188.	106.	128.	78.	130.	146.	211.
740	0.50	0.	17.	215.3	242.	178.	85.	109.	44.	112.	132.	202.
750	0.50	0.	18.	215.7	235.	167.	59.	86.	0.	88.	115.	193.
800	0.80	0.	19.	216.5	223.	147.	0.	13.	0.	11.	82.	175.
810	0.00	0.	21.	216.4	226.	149.	0.	0.	0.	0.	79.	177.
820	0.00	0.	21.	216.3	229.	152.	0.	0.	0.	0.	75.	178.
830	0.00	0.	21.	216.3	232.	154.	33.	5.	0.	0.	72.	179.
840	0.00	0.	21.	216.3	235.	157.	41.	26.	0.	0.	68.	180.
850	0.30	0.	21.	216.5	232.	149.	0.	0.	0.	0.	35.	174.
900	1.20	0.	21.	220.8	211.	114.	0.	0.	0.	0.	0.	0.
910	0.00	0.	56.	220.5	215.	119.	0.	0.	0.	0.	0.	0.
920	0.00	0.	56.	220.3	218.	123.	0.	0.	0.	0.	0.	0.
930	0.30	6.	56.	221.1	215.	116.	0.	0.	0.	0.	0.	0.
940	0.00	0.	56.	220.9	219.	121.	0.	0.	0.	0.	0.	0.
950	0.00	0.	56.	220.7	222.	125.	0.	0.	0.	0.	0.	0.
1000	0.70	40.	56.	221.1	211.	104.	0.	0.	0.	0.	0.	0.
1010	0.20	11.	56.	221.1	210.	101.	0.	0.	0.	0.	0.	0.
1020	0.00	0.	56.	220.9	214.	107.	0.	0.	0.	0.	0.	0.
1030	0.00	0.	56.	220.7	217.	113.	0.	0.	0.	0.	0.	0.
1040	0.40	19.	56.	221.1	212.	102.	0.	0.	0.	0.	0.	0.
1050	0.40	26.	56.	221.1	207.	91.	0.	0.	0.	0.	0.	0.
1100	0.30	19.	56.	221.1	205.	85.	0.	0.	0.	0.	0.	0.
1110	0.00	0.	56.	220.9	208.	93.	0.	0.	0.	0.	0.	0.
1120	0.00	0.	56.	220.7	212.	100.	0.	0.	0.	0.	0.	0.
1130	0.00	0.	56.	220.5	215.	106.	0.	0.	0.	0.	0.	0.
1140	0.00	0.	56.	220.2	219.	112.	0.	0.	0.	0.	0.	0.
1150	0.30	5.	56.	221.1	216.	106.	0.	0.	0.	0.	0.	0.
1200	0.00	0.	56.	220.9	219.	111.	0.	0.	0.	0.	0.	0.
1210	0.00	0.	56.	220.7	222.	116.	0.	0.	0.	0.	0.	0.
1220	0.00	0.	56.	220.5	226.	121.	0.	0.	0.	0.	0.	0.
1230	0.00	0.	56.	220.2	229.	125.	0.	0.	0.	0.	0.	0.
1240	0.00	0.	56.	220.0	232.	129.	0.	0.	0.	0.	0.	24.
1250	0.00	0.	47.	219.9	235.	133.	0.	0.	0.	0.	0.	40.
1300	0.00	0.	41.	219.8	237.	137.	0.	0.	0.	0.	0.	46.
1310	0.00	0.	38.	219.8	240.	140.	0.	0.	0.	0.	0.	50.
1320	0.00	0.	37.	219.8	243.	143.	25.	0.	0.	0.	0.	52.
1330	0.00	0.	37.	219.8	245.	146.	35.	0.	0.	0.	0.	54.
1340	0.00	0.	36.	219.7	248.	149.	42.	0.	0.	0.	0.	55.
1350	0.00	0.	36.	219.7	250.	153.	46.	0.	0.	0.	0.	57.
1400	0.00	0.	36.	219.7	252.	156.	50.	0.	0.	0.	0.	58.
1410	0.00	0.	36.	219.7	255.	158.	53.	0.	0.	0.	0.	59.
1420	0.00	0.	36.	219.7	257.	161.	55.	0.	0.	0.	0.	60.
1430	0.00	0.	36.	219.7	259.	163.	58.	0.	0.	0.	0.	61.
1440	0.00	0.	35.	219.6	261.	166.	60.	20.	0.	0.	0.	62.
1450	0.00	0.	35.	219.6	264.	168.	62.	34.	0.	0.	0.	66.
1500	0.00	0.	35.	219.5	266.	170.	65.	41.	0.	0.	0.	72.
1510	0.00	0.	34.	219.4	268.	173.	67.	45.	0.	0.	0.	78.
1520	0.00	0.	33.	219.3	270.	175.	69.	48.	0.	0.	0.	83.
1530	0.00	0.	33.	219.2	272.	177.	71.	51.	0.	0.	0.	87.
1540	0.00	0.	32.	219.1	274.	179.	73.	54.	0.	0.	0.	91.
1550	0.00	0.	32.	219.0	276.	182.	75.	56.	0.	0.	0.	94.
1600	0.00	0.	31.	219.0	277.	184.	76.	58.	0.	0.	0.	97.
1610	0.00	0.	31.	218.9	279.	186.	78.	59.	0.	0.	0.	100.

1620	0.00	0.	31.	218.8	281.	188.	80.	61.	0.	0.	0.	102.
1630	0.00	0.	30.	218.8	283.	190.	82.	62.	0.	0.	0.	104.
1640	0.00	0.	30.	218.8	284.	192.	84.	64.	0.	0.	0.	106.
1650	0.00	0.	30.	218.7	286.	194.	86.	65.	0.	0.	0.	108.
1700	0.00	0.	30.	218.7	288.	196.	87.	66.	0.	0.	0.	109.
1710	0.00	0.	29.	218.6	289.	198.	89.	67.	0.	0.	0.	111.
1720	0.00	0.	29.	218.6	291.	200.	91.	68.	0.	0.	0.	112.
1730	0.00	0.	29.	218.6	292.	202.	92.	70.	0.	0.	0.	113.
1740	0.00	0.	29.	218.5	294.	204.	94.	71.	0.	0.	0.	114.
1750	0.00	0.	29.	218.5	295.	206.	96.	72.	0.	0.	0.	115.
1800	0.00	0.	29.	218.5	297.	208.	97.	73.	0.	0.	0.	116.
1810	0.00	0.	29.	218.5	298.	210.	99.	74.	0.	0.	13.	117.
1820	0.00	0.	28.	218.4	300.	212.	101.	75.	0.	0.	25.	119.
1830	0.00	0.	28.	218.3	301.	214.	102.	76.	0.	0.	28.	121.
1840	0.00	0.	28.	218.3	302.	215.	104.	77.	0.	0.	30.	124.
1850	0.00	0.	28.	218.2	304.	217.	105.	78.	0.	0.	31.	126.
1900	0.00	0.	27.	218.1	305.	219.	107.	79.	0.	0.	32.	128.
1910	0.00	0.	27.	218.1	306.	221.	108.	80.	0.	0.	33.	131.
1920	0.00	0.	27.	218.0	308.	222.	110.	81.	0.	0.	34.	133.
1930	0.00	0.	27.	217.9	309.	224.	111.	81.	0.	0.	35.	135.
1940	0.00	0.	26.	217.9	310.	226.	113.	82.	0.	0.	35.	137.
1950	0.00	0.	26.	217.8	311.	227.	114.	83.	0.	0.	36.	138.
2000	0.00	0.	26.	217.7	313.	229.	116.	84.	0.	0.	36.	140.
2010	0.00	0.	26.	217.7	314.	230.	117.	85.	0.	0.	36.	142.
2020	0.00	0.	25.	217.6	315.	232.	119.	86.	0.	0.	37.	143.
2030	0.00	0.	25.	217.6	316.	233.	120.	87.	0.	0.	37.	145.
2040	0.00	0.	25.	217.5	317.	235.	121.	88.	0.	0.	38.	146.
2050	0.00	0.	25.	217.5	318.	236.	123.	88.	0.	0.	38.	148.
2100	0.00	0.	25.	217.4	320.	238.	124.	89.	0.	0.	38.	149.
2110	0.00	0.	25.	217.4	321.	239.	125.	90.	0.	0.	38.	151.
2120	0.00	0.	24.	217.4	322.	241.	127.	91.	0.	0.	39.	152.
2130	0.00	0.	24.	217.3	323.	242.	128.	92.	0.	0.	39.	153.
2140	0.00	0.	24.	217.3	324.	244.	129.	92.	0.	0.	39.	155.
2150	0.00	0.	24.	217.2	325.	245.	131.	93.	0.	0.	40.	156.
2200	0.00	0.	24.	217.2	326.	246.	132.	94.	0.	0.	40.	156.
2210	0.00	0.	24.	217.2	327.	248.	133.	95.	0.	0.	40.	157.
2220	0.00	0.	23.	217.1	328.	249.	135.	96.	0.	0.	40.	158.
2230	0.00	0.	23.	217.1	329.	250.	136.	96.	0.	0.	40.	159.
2240	0.00	0.	23.	217.1	330.	251.	137.	97.	0.	0.	41.	160.
2250	0.00	0.	23.	217.0	331.	252.	138.	98.	0.	0.	41.	161.
2300	0.00	0.	23.	217.0	332.	253.	140.	99.	0.	0.	41.	162.
2310	0.00	0.	23.	217.0	333.	255.	141.	99.	0.	0.	41.	162.
2320	0.00	0.	23.	217.0	334.	256.	142.	100.	0.	0.	41.	163.
2330	0.00	0.	23.	216.9	335.	257.	143.	101.	0.	0.	41.	164.
2340	0.00	0.	23.	216.9	336.	258.	144.	101.	0.	13.	41.	164.
2350	0.00	0.	23.	216.9	337.	260.	146.	102.	0.	12.	44.	165.
2400	0.00	0.	22.	216.8	338.	261.	147.	103.	0.	12.	46.	166.

Percentage of rainfall becoming surface runoff is 12.3

REFERENCES

Anderson, M.G. and Burt, T.P. (1978). The role of topography in controlling throughflow generation. *Earth Surface Processes 3*: 331-344.

Bear, J. (1972). 'Dynamics of Fluids in Porous Media'. Elsevier, New York, 764 pp.

Betson, R.P. (1964). What is watershed runoff? *Journal of Geophysical Research 69*: 1541-1552.

Becker, A. (1974). Applied principles in catchment simulation. *In* Mathematical models in hydrology. Proceedings of the Warsaw Symposium, 1971. Vol. 2. I.A.H.S. Publication No. 101 pp. 762-774.

Betson, R.V. and Ardis, C.V. Jr. (1978). Implications for modelling surface-water hydrology. *In* 'Hillslope Hydrology', Kirkby, M.J. (ed.). John Wiley and Sons, Chichester, pp. 295-323.

Beven, K. (1978). The hydrological response of headwater and sideslope areas. *Hydrology Science Bulletin 23*: 419-437.

Beven, K. and Germann, P. (1982). Macropores and water flow in soils. *Water Resources Research 18*: 1311-1325.

Bonnell, M., Henricks, M.R., Imeson, A.C. and Hazelhoff, L. (1984). the generation of storm runoff in a forested clayey drainage basin in Luxembourg. *Journal of Hydrology 71*: 53-77.

Chow, V.T. (ed.). (1964). 'Handbook of Applied Hydrology'. McGraw Hill, New York, 1418 pp.

USDA, Soil Conservation Service (1972). National Engineering Handbook, Hydrology, Section 4, 548 pp.

Clarke, R.T. (1973). A review of some mathematical models used in hydrology, with observations on their calibration and use. *Journal of Hydrology 19*: 1-20.

Crawford, N.H. and Linsley, R.K. (1962). The synthesis of continuous streamflow hydrographs on a digital computer. Department of Civil Engineering, Stanford University Technical Report No. 12.

Crawford, N.H. and Linsley, R.K. (1966). Digital simulation in hydrology: Stanford Watershed Model IV. Department of Civil Engineering, Stanford University Technical Report No. 39.

Dubreuil, P.L. (1985). Review of field observations of runoff generation in the tropics. *Journal of Hydrology 80*: 237-264.

Dunin, F.X. (1976). Infiltration: Its simulation for field conditions. *In* 'Facets of Hydrology', Rodden, J.C. (ed.). John Wiley and Sons, London. pp. 199-227.

Dunne, T. (1978). Field studies of hillslope flow processes. *In* 'Hillslope Hydrology', Kirkby, M.J. (ed.). John Wiley and Sons, Chichester. pp. 227-293.

Dunne, T. and Black, R.D. (1970a). An experimental investigation of runoff production in permeable soils. *Water Resources Research 6*: 478-490.

Dunne, T. and Black, R.D. (1970b). Partial area contributions to storm runoff in a small New Zealand watershed. *Water Resources Research 6*: 1296-1311.

England, C.B. and Onstad, C.A. (1968). Isolation and characterization of hydrologic response units within agricultural watersheds. *Water Resources Research 4*: 73-77.

Engman, E.T. and Rogowski, A.S. (1974). A partial area model for storm flow synthesis. *Water Resources Research 10*: 464-472.

Freeze, R.A. (1972a). Role of subsurface flow in generating surface runoff. 1. Base flow contributions to channel flow. *Water Resources Research 8:* 609-623.

Freeze, R.A. (1972b). Role of subsurface flow in generating surface runoff. 2. Upstream source areas. *Water Resources Research 8:* 1272-1283.

Freeze, R.A. (1980). A stochastic-conceptual analysis of rainfall-runoff processes on a hillslope. *Water Resources Research 16*: 391-408.

Green, R.E. and Corey, J.C. (1971). Calculation of hydraulic conductivity: A further evaluation of some predictive models. *Soil Science Society America Proceedings 35:* 3-8.

Hammermeister, D.P., Kling, G.F. and Vomocil, J.A. (1982). Perched water tables on hillslides in Western Oregon. I. Some factors affecting their development and longevity. *Soil Science Society of America Journal 46:* 811-818.

Hammermeister, D.P., Kling, G.F. and Vomocil, J.A. (1982). II. Preferential downslope movement of water and anions. *Soil Science Society of America Journal 46:* 819-826.

Harr, R.D. (1977). Water flux in soil and subsoil on a steep forested slope. *Journal of Hydrology 33:* 37-58.

Hewlett, J.D. and Hibbert, A.R. (1963). Moisture and energy conditions within a sloping soil mass during drainage. *Journal of Geophysical Research 68:* 1081-1087.

Hewlett, J.D. and Hibbert, A.R. (1967). Factors affecting the response of small watersheds to precipitation in humid areas. *In* 'Forest Hydrology', Sopper, W.A. and Lull, H.W. (eds). Pergamon Press.

Hewlett, J.D. and Troendle, C.A. (1975). Non-point and diffused water sources: A variable source area problem. Proceedings of Symposium on Watershed Management. American Society of Civil Engineering, New York, pp. 21-46.

Hillel, D. (1971). 'Soil and water, physical principles and processes'. Academic Press, New York, 228 pp.

Hillel, D. (1975). Some criteria for comprehensive modelling of transport phenomena in the soil-plant-atmosphere continuum. *In* Computer simulation of water resources systems. Vansteenkiste, G.C. (ed.). North Holland, Amsterdam. pp. 121-130.

Hillel, D. (1977). Computer simulation of soil-water dynamics; a compendium of recent work. International Development Research Centre, Ottawa, 214 pp.

Holtan, H.N. (1965). A model for computing watershed retention from soil parameters. *Journal of Soil and Water Conservation 20:* 91-94.

Holtan, H.N. and Lopez, N.C. (1971). USDAHL - 70 Model of watershed hydrology. USDA-ARS Technical Bulletin No. 1435.

Holtan, H.N., Stiltner, G.J., Henson, W.H. and Lopez, N.C. (1975). USDAHL - 74 revised model of watershed hydrology. USDA-ARS Technical Bulletin No. 1518.

Horne, D.J. (1985). Some consequences of mole draining a yellow-grey earth under pasture. Ph.D. Thesis, Massey University, 227 pp.

Horton, H.N. and Hawkins, R.H. (1965). Flow path of rain from the soil surface to the water table. *Soil Science 100:* 337-383.

Horton, R.E. (1933). The role of infiltration in the hydrologic cycle. *Transactions of the American Geophysics Union 14:* 446-460.

Huggins, L.F. and Monke, E.J. (1966). The mathematical simulation of the hydrology of small watersheds. Technical Report 1. Water Resources Research Centre, Purdue University, Indiana, 130 pp.

Huggins, L.F. and Monke, E.J. (1968). A mathematical model for simulating the hydrologic response of a watershed. *Water Resources Research 4:* 529-539.

Hursh, C.R. (1944). Reports on Hydrology - 1944 - Appendix B - Report on sub-committee on subsurface flow. *Transactions of the American Geophysics Union 25:* 743-746.

Hursh, C.R. and Fletcher, P.W. (1942). Soil profile as a natural reservoir. *Soil Science Society of America Proceedings 7:* 480-486.

Hursh, C.R. and Hoover, M.D. (1941). Soil profile characteristics pertinent to hydrological studies in the Southern Appalachians. *Soil Science Society of America Proceedings 6:* 414-422.

James, L.D. (1972). Hydrologic modeling, parameter estimation, and watershed characteristics. *Journal of Hydrology 7:* 283-307.

Kirkby, M.J. and Chorley, R.J. (1967). Throughflow, overland flow and erosion. *Bulletin of the International Association of Scientific Hydrology 12:* 5-21.

Kisiel, C.C. (1971). Efficiency of parameter and state estimation methods in relation to models of lumped and distributed hydrologic systems. *In* Systems Approach to Hydrology. Proceedings of the 1st Bilateral US-Japan Seminar in Hydrology, Honolulu (1971). Water Resources Publications, Fort Collins, Colorado, pp. 246-272.

Mandelbrot, B.B. (1970). Comment on 'Stochastic models in hydrology' by Scheidegger, A.E. *Water Resources Research 6:* 1791.

Mejia, J.M. and Rodriguez, Iturbe (1974). On the synthesis of random field sampling from the spectrum: An application to the generation of hydrologic spatial processes. *Water Resources Research 10*: 705-711.

Merva, G.E., Brazee, R.D., Schwab, G.O. and Curry, R.B. (1969). A proposed mechanics for the investigation of surface runoff from small watersheds. I. Development. *Water Resources Research 5:* 76-83.

Mosley, M.P. (1982). The effect of a New Zealand beech forest canopy on the kinetic energy of water drops and on surface erosion. *Earth Surface Processes and Landforms 7:* 103-107.

Musgrave, G.W. (1955). How much of the rain enters the soil? *In* 'Water' USDA Yearbook, 1955, pp. 151-159.

Musgrave, G.W. and Holtan, H.N. (1964). Infiltration. *In* 'Handbook of Applied Hydrology'. Chow, V.T. (ed.). McGraw-Hill, New York, Section 12.

Ören, T.I. (1979). Concepts for advanced computer assisted modelling. *In* 'Methodology in systems modelling and simulation. Zeigler, B.P., Elzas, M.S., Klir, G.J. and Ören, T.I. (eds). North Holland, Amsterdam pp. 29-55.

Palkovics, W.E. and Petersen, G.W. (1977). Contribution of lateral soil water movement above a fragipan to streamflow. *Soil Science Society of America Journal 41:* 394-400.

Parlange, J.Y. (1972). Analytical theory of water movement in soils. 'Joint symposium of fundamentals of transport phenomena in power media', University of Guelph, Ontario, August 1972. pp. 222-236.

Philip, J.R. (1969). Theory of infiltration. *Advances in Hydroscience 5:* 215-296.

Philip, J.R. (1975). Some remarks on science and catchment prediction. *In* 'Prediction in Catchment Hydrology'. Chapman, T.G. and Dunin, F.X. (eds.). Australian Academy of Science, pp. 23-30.

Pilgrim, D.H., Huff, D.D. and Steele, J.D. (1978). A field evaluation of subsurface and surface runoff. II. Runoff processes. *Journal of Hydrology 38*: 319-341.

Richards, L.A. (1931). Capillary conduction of liquids through porous mediums. *Physics 1:* 318-333.

Rogowski, A.S. (1971). Watershed physics: Model of the soil moisture characteristic. *Water Resources Research 7:* 1575-1582.

Rogowski, A.S. (1972). Estimation of the soil moisture characteristic and hydraulic conductivity: Comparison of models. *Soil Science 114:* 423-429.

Rovey, E.W., Woolhiser, D.A. and Smith, R.E. (1977). A distributed kinematic model of upland watersheds. Hydrology paper No. 93. CSU, Fort Collins, 52 pp.

Scotter, D.R., Clothier, B.E. and Corker, R.B. (1979). Soil water in a fragiaqualf. *Australian Journal of Soil Research 17:* 443-453.

Scotter, D.R., Clothier, B.E., and Harper, E.R. (1982). Measuring saturated hydraulic conductivity and sorptivity using twin rings. *Australian Journal of Soil Research 20*: 295-304.

Smith, R.E. (1972). The infiltration envelope: Results from a theoretical infiltrometer. *Journal of Hydrology 17*: 1-21.

Smith, R.E. (1982). Rational models of infiltration hydrodynamics. *In* 'Modeling Components of Hydrologic Cycle'. Singh, V.P. (ed.). Water Resources Publications, Colorado, pp. 107-126.

Smith, R.E. and Chery, D.L. (1973). Rainfall excess model from soil water flow theory. *Journal of the Hydraulics Division Proceedings ASCE 99 (H79):* 1337-1351.

Smith, R.E. and Parlange, J.Y. (1978). A parameter-efficient hydrologic infiltration model. *Water Resources Research 14*: 533-538.

Smith, R.E. and Woolhiser, D.A. (1971). Overland flow on an infiltrating surface. *Water Resources Research 7:* 899-913.

Ward, R.C. (1984). On the response to precipitation of headwater streams in humid areas. *Journal of Hydrology 74:* 171-189.

Whipkey, R.Z. (1965). Subsurface stormflow from forested slopes. *Bulletin of International Association of Hydrological Science 10:* 64-85.

Zaslavsky, D. and Rogowski, A.S. (1969). Hydrologic and morphologic implications of anisotrophy and infiltration in soil profile development. *Soil Science Society of America Proceedings 33:* 594-599.

Zeigler, B.P. (1976). Theory of modelling and simulation. John Wiley and Sons, New York.